

Nicotianamine Functions in the Phloem-Based Transport of Iron to Sink Organs, in Pollen Development and Pollen Tube Growth in *Arabidopsis*

Mara Schuler,^a Rubén Rellán-Álvarez,^{b,1} Claudia Fink-Straube,^c Javier Abadía,^b and Petra Bauer^{a,2}

^aDepartment of Biosciences–Botany, Saarland University, D-66123 Saarbrücken, Germany

^bDepartment of Plant Nutrition, Aula Dei Experimental Station (Consejo Superior de Investigaciones Científicas), E-50080 Zaragoza, Spain

^cLeibniz Institute for New Materials, D-66123 Saarbrücken, Germany

The metal chelator nicotianamine promotes the bioavailability of Fe and reduces cellular Fe toxicity. For breeding Fe-efficient crops, we need to explore the fundamental impact of nicotianamine on plant development and physiology. The quadruple *nas4x-2* mutant of *Arabidopsis thaliana* cannot synthesize any nicotianamine, shows strong leaf chlorosis, and is sterile. To date, these phenotypes have not been fully explained. Here, we show that sink organs of this mutant were Fe deficient, while aged leaves were Fe sufficient. Upper organs were also Zn deficient. We demonstrate that transport of Fe to aged leaves relied on citrate, which partially complemented the loss of nicotianamine. In the absence of nicotianamine, Fe accumulated in the phloem. Our results show that rather than enabling the long-distance movement of Fe in the phloem (as is the case for Zn), nicotianamine facilitates the transport of Fe from the phloem to sink organs. We delimit nicotianamine function in plant reproductive biology and demonstrate that nicotianamine acts in pollen development in anthers and pollen tube passage in the carpels. Since Fe and Zn both enhance pollen germination, a lack of either metal may contribute to the reproductive defect. Our study sheds light on the physiological functions of nicotianamine.

INTRODUCTION

Fe deficiency is one of the most prevalent nutrient deficiencies threatening human health in the world, affecting approximately two billion people (de Benoist et al., 2008). One of the most effective strategies to combat human malnutrition is breeding major staple food crops enriched in bio-available micronutrients. The metal chelator and nonproteinogenic amino acid nicotianamine (NA) is known to bind a range of metal ions, including Fe²⁺, Fe³⁺, and Zn²⁺ (Anderegg and Ripperger, 1989; Scholz et al., 1992; von Wiren et al., 1999; Reichman and Parker, 2002; Schmiedeberg et al., 2003; Weber et al., 2006; Rellán-Álvarez et al., 2008; Nishiyama et al., 2012). NA promotes high Fe content and Fe bioavailability in cereal grains (Lee et al., 2009; Zheng et al., 2010). NA is produced by NA synthase (NAS) (Shojima et al., 1989, 1990; Herbik et al., 1999; Higuchi et al., 1999), and NAS genes have been recognized as valuable targets in the generation of micronutrient-enriched crops (Douchkov et al., 2005; Cassin et al., 2009; Lee et al., 2009; Wirth et al., 2009;

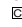
Zheng et al., 2010; Johnson et al., 2011). Indeed, alterations of NAS gene activities affect NA contents, resulting in phenotypical changes related to uptake and distribution of Fe (Scholz et al., 1992; Douchkov et al., 2001, 2005; Takahashi et al., 2003; Klatte et al., 2009) as well as of Zn (Deinlein et al., 2012; Haydon et al., 2012). Altering NAS activities and NA levels are therefore among the most promising biotechnological biofortification approaches.

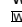
For optimal exploitation of NA alterations, it is important to better understand the action and functions of this molecule in plants. NA has been found in the phloem sap (Schmidke et al., 1999; Nishiyama et al., 2012), and it was also immunologically detected inside vacuoles at the root tip and in the root stele (Pich et al., 1997). Recent reports uncovered that inside the vacuole, NA functions in Zn chelation (Haydon et al., 2012) and that the complex Zn-NA occurs in the phloem sap (Nishiyama et al., 2012). Inside the phloem, which has neutral pH values, the stability of the Fe-NA complexes seems optimal, and it was proposed that inside the phloem sap NA might chelate Fe (von Wiren et al., 1999; Reichman and Parker, 2002; Weber et al., 2006; Rellán-Álvarez et al., 2008). NA prevents Fe precipitation and promotes the delivery of Fe to its target sites (Becker et al., 1995), and in addition, it minimizes Fe toxicity as the chelation prevents radical production via the Fenton reaction (Hell and Stephan, 2003). These essential and protective functions of NA are important for cellular metal homeostasis in all tissues. Besides that, NA is a mobile compound in the plant that is synthesized in roots, leaves, and flowers and can be transported to other organs from there (Scholz et al., 1992). Thus, NA is also involved in the long-distance distribution of metals in plants. Recent proof was given that NA is involved in the long-distance

¹ Department of Plant Biology, Carnegie Institution for Science, Stanford, CA 94305.

² Address correspondence to p.bauer@mx.uni-saarland.de.

The author responsible for distribution of materials integral to the findings presented in this article in accordance with the policy described in the Instructions for Authors (www.plantcell.org) is: Petra Bauer (p.bauer@mx.uni-saarland.de).

 Some figures in this article are displayed in color online but in black and white in the print edition.

 Online version contains Web-only data.

www.plantcell.org/cgi/doi/10.1105/tpc.112.099077

transport of Zn from root to shoot since plants depleted in NA or with NA trapped in the root had lower Zn levels in their leaves (Klatte et al., 2009; Deinlein et al., 2012; Haydon et al., 2012). Due to the likelihood of Fe-NA complex formation in the phloem, NA might function in the long-distance transport of Fe. However, evidence for this is lacking, and NA-depleted plants have increased Fe levels in their shoots (Takahashi et al., 2003; Klatte et al., 2009). Short-distance translocation of NA across membranes is achieved through the activities of various transport proteins that may transport free NA (Haydon et al., 2012) or metal-NA chelates, the latter of which includes certain members of the YELLOW STRIPE1-LIKE (YSL) oligopeptide transporter family (Curie et al., 2001, 2009). *Arabidopsis thaliana* YSL1, YSL2, and YSL3 are expressed in vascular bundles and are induced by Fe (DiDonato et al., 2004; Schaaf et al., 2005). These YSL transporters presumably mediate the lateral movement of Fe-NA from the xylem and phloem and are involved in reproduction and seed Fe loading (Le Jean et al., 2005; Waters et al., 2006; Chu et al., 2010). In rice (*Oryza sativa*), OsYSL2 may contribute to the loading of Fe-NA into the phloem (Koike et al., 2004; Ishimaru et al., 2010).

To uncover novel functions of NA and to investigate its effects on whole-plant physiology, we generated mutants for NA in the model plant *A. thaliana*. Many genes and mutants are being characterized in this species, and they serve as tools in our investigation of NA functions. *A. thaliana* has four *NAS* genes, *NAS1*, *NAS2*, *NAS3*, and *NAS4* (Bauer et al., 2004), and we have been able to generate two quadruple mutants, *nas4x-1* and *nas4x-2*, by combining different mutant *nas* T-DNA insertion alleles (Klatte et al., 2009). Both mutants harbor the full loss-of-function alleles *nas1-1*, *nas3-1*, and *nas4-1*, while they differ at their *nas2* allele. *nas4x-1* plants have the leaky *nas2-1* allele with residual *NAS* activity, leading to reduced NA levels in leaves of the vegetative stage and seeds and no NA in leaves of the reproductive stage (RS). The reduced NA levels are sufficient to sustain plant viability and reproduction. In *nas4x-1* plants, higher Fe amounts are transported to leaves despite low NA levels, and *nas4x-1* leaves show symptoms of Fe deficiency and sufficiency (Klatte et al., 2009). The increased uptake and transport of Fe is due to long-distance signaling of Fe deficiency from leaves to roots. *nas4x-1* plants have a reduced Zn content in leaves and flowers (Klatte et al., 2009). Using *nas4x-1*, we demonstrated a correlation between NA and Fe contents in seeds (Klatte et al., 2009) and were able to establish gene expression profiles in response to altered metal homeostasis (Schuler et al., 2011). The *nas4x-2* mutant, on the other hand, has the full loss-of-function *nas2-2* allele and does not produce any NA. *nas4x-2* plants are growth-retarded, highly chlorotic, and sterile, showing that NA is essential throughout plant development in *A. thaliana* (Klatte et al., 2009).

Several questions remained unanswered to date regarding the physiological and developmental functions affected by the absence of NA. The hypothesis that NA facilitates the long-distance transport of Fe needs further support, since the transport of Fe as a citrate complex in the xylem takes place whether or not NA is present. The contradictory finding that leaves of NA-reduced plants show signs of Fe deficiency and Fe sufficiency (Klatte et al., 2009) was not sufficiently investigated. Moreover, the functions of NA during specific processes of plant reproduction need to be characterized.

In this study, we used the full loss-of-function and NA-free *nas4x-2* mutant to show that NA is involved in long-distance Fe transport to sink organs and that sink organs, including young leaves and flowers, are Fe deficient. We show that NA is needed for the mobilization of Fe from the phloem rather than in long-distance transport itself. We also dissect the reproductive failure of the quadruple mutant and show that NA is essential for pollen production and pollen tube passage. Taken together, our results shed light on the diverse roles of NA in metal homeostasis.

RESULTS

Leaf Chlorosis Phenotypes, Fe Contents, and Fe-Dependent Gene Expression Varied with Age in *nas4x-2* Leaves

nas4x-2 mutant plants have a strong interveinal leaf chlorosis. This chlorosis can be rescued by the application of 5 μ M NA onto leaf surfaces, showing that the leaf chlorosis is caused by the lack of NA. When studying *nas4x-2* plants, we noted that the strength of leaf chlorosis phenotypes differed in young and old leaves. Since the loss of NA is associated with a higher content of Fe in leaves, we hypothesized that perhaps the accumulation and localization of Fe in *nas4x-2* leaves varied with age. To study this aspect further, we separated young, middle-aged, and aged leaves and then analyzed leaf chlorosis, Fe contents, and ferritin (*FER1*) gene expression. First, we documented the leaf chlorosis phenotypes at different growth stages (Figure 1). The leaf chlorosis of *nas4x-2* was apparent 2 to 3 weeks after germination, in the first leaves at the early vegetative stage (EVS). These leaves were young and not fully expanded and showed a strong yellow interveinal leaf chlorosis (young leaves, marked “y” in Figures 1B and 1C). Leaf chlorosis was also strong in the youngest leaves of plants grown for 4 to 5 weeks (up to the late vegetative stage [LVS]) and 7 to 9 weeks (when plants had reached the RS) (Figures 1A to 1C). Just after their expansion and maturation, the leaves of the LVS and RS stages, now termed middle-aged (marked “m” in Figures 1B and 1C), altered their chlorosis phenotype. Leaf areas turned light green to green, while the leaf veins stayed dark green. Aged leaves in the RS appeared nearly normally green like wild-type leaves (marked “a” in Figures 1B and 1C). The appearance of the strong interveinal leaf chlorosis in young leaves of *nas4x-2* and its nearly full recovery during maturation and aging points to a stronger Fe deficiency in young leaves compared with middle-aged and aged leaves. We hypothesize that NA was needed for Fe acquisition by young leaves, whereas maturing leaves were rescued by alternative Fe transport pathways.

In our previous study, we found an elevated Fe content in the whole rosette of *nas4x-1* mutants compared with wild-type plants at the reproductive but not at the vegetative stage (Klatte et al., 2009). From these observations, we deduced that aged leaves of NA-reduced plants had acquired high levels of Fe. However, in these previous experiments, we did not discriminate between young and aged leaves. To test our hypothesis that different Fe nutrition routes may exist in young and aged leaves, we determined the Fe contents in leaves of different ages harvested at the EVS, LVS, and RS. We found that all leaf types of *nas4x-2* plants showed significant changes in Fe contents compared with the wild type (Figure 2A). Young leaves of all growth stages showed

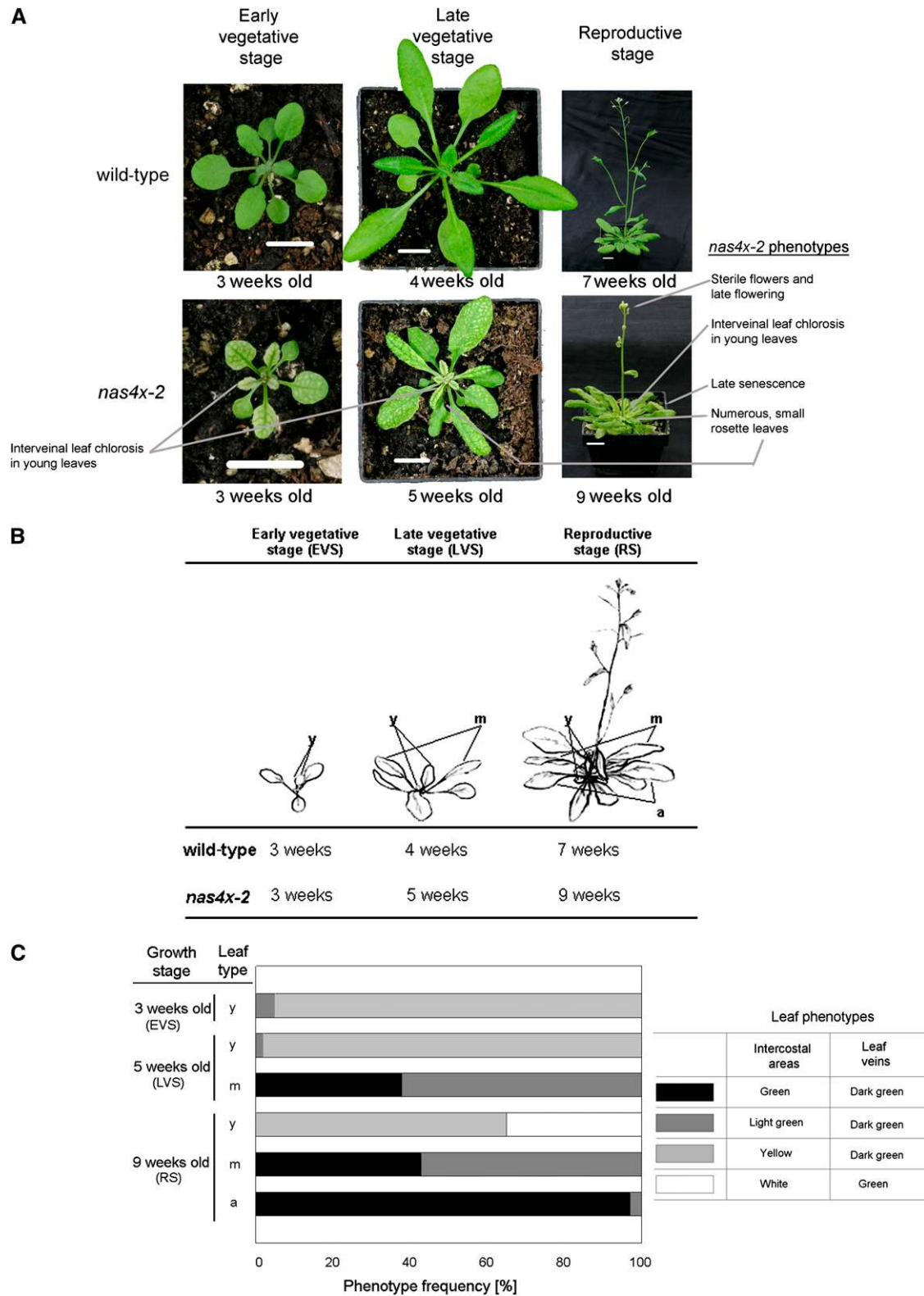


Figure 1. *nas4x-2* Mutants Showed Multiple Morphological Phenotypes.

Growth phenotypes of wild-type and *nas4x-2* plants during EVS, LVS, and RS growth stages. Plants were grown on soil under long-day conditions over a time course of up to 7 weeks (the wild type) and 9 weeks (*nas4x-2*). Note that *nas4x-2* plants were growth retarded compared with the wild type.

a decrease in Fe contents in *nas4x-2* plants compared with wild-type leaves, while middle-aged and aged *nas4x-2* leaves showed an increase in Fe contents (Figure 2A). These results confirm a correlation between leaf chlorosis phenotypes and Fe content.

We further analyzed the expression levels of the ferritin gene *FER1*, a marker for Fe excess and the associated oxidative stress (Petit et al., 2001; Ravet et al., 2009) and of the putative NA transporter gene *YSL1*, which is upregulated by Fe supply in leaves (Waters et al., 2006). We expected that the young chlorotic leaves of *nas4x-2* plants with low Fe levels may not show an induction of *FER1* and *YSL1*, while middle-aged and aged leaves with high Fe contents may show increased transcript levels due to local Fe overload and oxidative stress. Indeed, we found that *FER1* and *YSL1* were highly induced in middle-aged and aged *nas4x-2* leaves compared with the wild type, whereas their expression remained unchanged or was lower in young leaves (Figures 2B and 2C). This finding confirmed a correlation between *FER1* and *YSL1* expression levels, Fe content, and leaf chlorosis phenotypes. Moreover, *nas4x-2* plants had elevated levels of *IRON-REGULATED TRANSPORTER1* (*IRT1*), *FERRIC REDUCTASE OXIDASE2* (*FRO2*), and *FER-LIKE IRON DEFICIENCY-INDUCED TRANSCRIPTION FACTOR* (*FIT*) expression in roots (see Supplemental Figure 1 online), as we previously showed for *nas4x-1* (Klatte et al., 2009). The upregulation of Fe acquisition in *nas4x-2* roots explains the overall increased Fe contents in *nas4x-2* shoots.

Taken together, these results show that young leaves are Fe deficient in the absence of NA, while middle-aged and aged leaves are Fe sufficient.

Citrate and NA Play Partially Redundant Roles in the Root-to-Leaf Translocation of Fe

From the previous experiments, it can be deduced that NA is involved in the translocation of Fe from the root to the young leaves. On the other hand, alternative Fe transport routes apparently act to supply Fe to middle-aged and aged leaves. Citrate is the preferred Fe chelator at the typical pH values of xylem, while in the phloem sap, NA is supposed to be the main candidate for Fe chelation (Rellán-Alvarez et al., 2008, 2011). We have previously shown that ligand exchange reactions between citrate and NA occur almost instantaneously (Rellán-Alvarez et al., 2008). In fact, these rapid ligand exchange reactions are thought to happen whenever Fe complexes move from one compartment to another that differs in pH value. Depending on the actual pH value of xylem and phloem sap and on the available amount of both Fe complexing molecules, both chelators may complement each other's function in Fe transport. *frd3* mutant

plants with a nonfunctional citrate transporter gene have citrate levels that are 40% less than those of the wild type in the xylem and accumulate Fe in the root central cylinder (Rogers and Guerinot, 2002; Green and Rogers, 2004; Durrett et al., 2007). Due to the low occurrence of Fe-citrate translocation to leaves, Fe deficiency signals are emitted that enhance Fe acquisition mechanisms in roots, resulting in metal accumulation in *frd3* plants. The *frd3* mutant is therefore a good tool to investigate citrate-mediated transport of Fe. Interestingly, it was reported that *frd3* mutants have a twofold increase in NA levels (Rogers and Guerinot, 2002). Moreover, in a previous microarray analysis, we observed that *FRD3* is induced in *nas4x-1* mutants compared with wild-type plants (Schuler et al., 2011). To investigate whether *FRD3* and *NAS* regulation are linked, we analyzed the expression of these genes in the two mutants, *frd3* and *nas4x-2*. We found that *FRD3* was induced 12-fold in *nas4x-2* roots (Figure 3A), whereas *NAS1* was induced 14-fold, *NAS2* 50-fold, and *NAS4* fourfold in *frd3* roots compared with the wild type (Figure 3B; note that *NAS3* is not expressed in roots). On the other hand, we could not find any changes in gene expression levels in leaves of both mutants (Figures 3A and 3B), showing that NA and citrate effects were confined to roots. These results support the notion that plants compensate the lack of citrate or NA by promoting the synthesis of the other chelator. Citrate and NA may therefore act, at least partially, in a redundant manner in the long-distance transport of Fe from roots to leaves.

To investigate this hypothesis, we studied the effects of a simultaneous loss of citrate and NA. We suspected that this situation may lead to a persisting strong leaf chlorosis. We therefore crossed the *frd3* mutant (*frd3-3*) with *nas4x-2* and identified a quintuple *frd3 nas4x-2* mutant. The *frd3-3* allele contains a stop codon that disrupted the open reading frame so that functional *FRD3* is not produced (Rogers and Guerinot, 2002). At first, we characterized the leaf chlorosis and growth phenotypes of the quintuple mutant in the three different growth stages analyzed above and documented the phenotypes compared with *frd3*, *nas4x-2*, and the wild type. We found that *frd3 nas4x-2* mutants developed a severe interveinal leaf chlorosis, which intensified with age and was stronger than that of the *nas4x-2* plants (Figures 4A and 4B). Furthermore, aged leaves of *frd3 nas4x-2* mutants turned only light green, in contrast with aged *nas4x-2* leaves, which nearly fully recovered from the initial chlorosis (cf. Figures 4B and 1C). The stronger phenotype of *frd3 nas4x-2* compared with *frd3* and *nas4x-2* alone is indicative of a synergistic (rather than additive) effect of the two mutations on leaf chlorosis, so that the loss of NA or citrate is partially complemented by the other chelator.

Next, we compared the Fe content of *frd3 nas4x-2* plants grown to the RS with that of the single mutants. The young leaves

Figure 1. (continued).

(A) Photographs of morphological phenotypes. Bars = 1 cm.

(B) Schematic representation of the three growth stages analyzed. For molecular-physiological analysis, young expanding (y), middle-aged fully expanded (m), and aged, nearly senescent (a) leaves were harvested.

(C) Comparison of the leaf chlorosis phenotypes of *nas4x-2* leaves at different growth stages, showing rescue of leaf chlorosis during maturation of the leaves. The different leaf chlorosis phenotypes are described, and the percentage of leaves manifesting these phenotypes is shown. Control, wild-type leaves of all stages were green (data not shown).

[See online article for color version of this figure.]

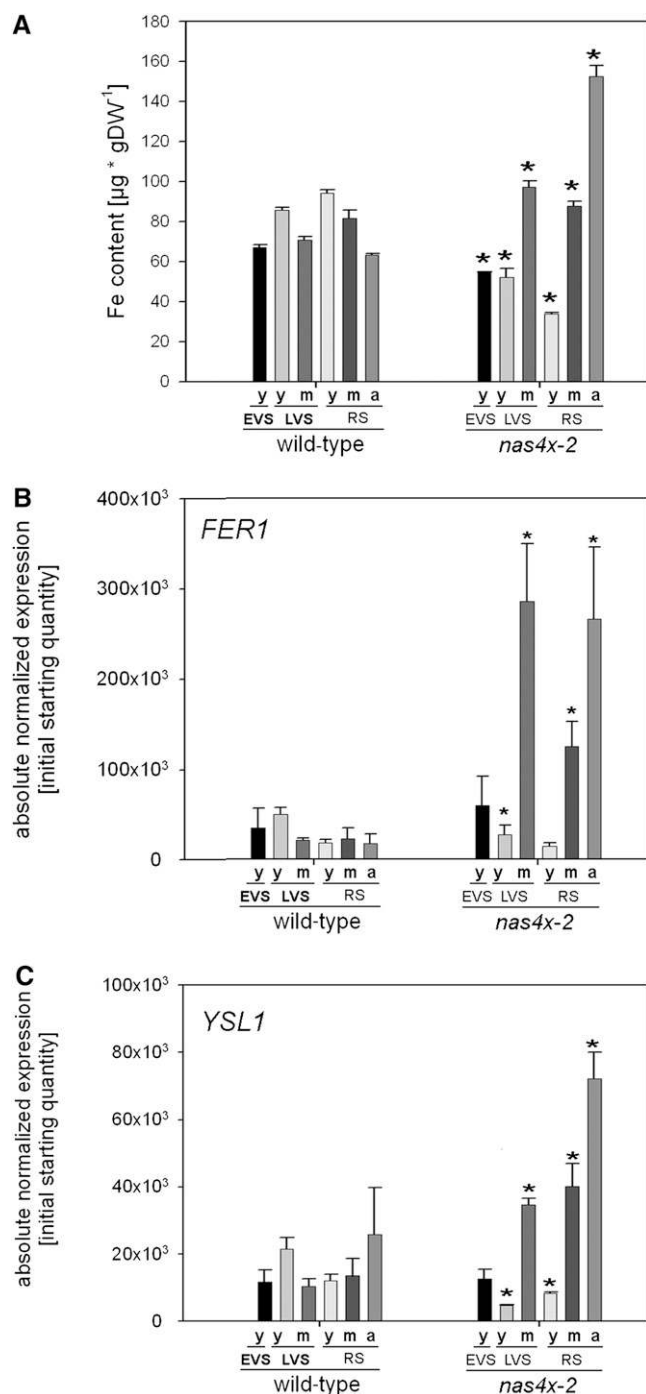


Figure 2. Young, Middle-Aged, and Aged Rosette Leaves of *nas4x-2* Differed in Fe Content and in *FER1* and *YSL1* Expression.

Plants were grown on soil under long-day conditions up to EVS, LVS and RS; young (y), middle-aged (m), and aged (a) rosette leaves were harvested for analysis (see phenotypes in Figure 1).

(A) Fe contents of leaves, showing that Fe contents were reduced in young leaves of *nas4x-2* plants, but increased in middle-aged and aged leaves of *nas4x-2* in all analyzed stages ($n = 4$; * $P < 0.05$ for the comparison *nas4x-2* versus the wild type). DW, dry weight.

of the quintuple mutant showed low Fe contents, as in *nas4x-2*, compared with the wild type and *frd3* (Figure 5A). Fe contents of middle-aged and aged leaves of *frd3 nas4x-2* plants were lower than those of *nas4x-2* leaves (Figure 5A). This finding indicates that the reduction of citrate levels in the *frd3 nas4x-2* quintuple mutant reduced Fe translocation to the middle-aged and aged leaves. This observation could also be confirmed using the Perl's Fe stain method (see Supplemental Figure 2 online). On the other hand, roots of *frd3 nas4x-2* mutants had high levels of Fe staining and Fe contents, like *frd3* but in contrast with *nas4x-2* and the wild type (see Supplemental Figures 3A and 3B online). Taken together, *NAS* genes and NA seem to be important for Fe transport to young leaves, as deduced from the reduced Fe content in leaves with a *nas4x-2* background. *FRD* and citrate are important for Fe transport to aged leaves, leading to elevated Fe contents in aged leaves of *nas4x-2* but not of the quintuple mutant. Thus, NA is important for phloem-fed tissues (young leaves), while citrate is important for xylem-fed tissues (aged leaves).

To provide evidence for the compensatory effect of citrate in the root to leaf Fe translocation in *nas4x-2* mutants, we analyzed citrate concentrations in the xylem sap. We also included measurements of other putative Fe ligands, namely malate, succinate, and 2-oxoglutarate. We observed that, as expected, *frd3* showed a significant decrease (nearly 50%) in xylem sap citrate concentration compared with that of the wild type (Figure 5B). *nas4x-2* xylem sap showed a fourfold increase in citrate concentrations compared with the wild type, which shows a compensatory increase of citrate in *nas4x-2* plants (Figure 5B). The citrate level of *frd3 nas4x-2* mutants was again decreased and similar to the levels found in *frd3* single mutants (Figure 5B). No major differences were obtained for malate, 2-oxoglutarate, and succinate concentrations (see Supplemental Figure 4 online) in the xylem of the mutants when compared with those of the wild type, indicating that these carboxylates were not involved in the compensation of Fe transport in the xylem of *nas4x-2* mutants.

Taken together, these results provide evidence for crosstalk between NA- and citrate-mediated Fe translocation to leaves. Due to internal plant Fe deficiency signaling, these pathways were activated upon reduced function of each other. While NA promoted long-distance Fe translocation to young leaves, citrate mediated transport to middle-aged and aged leaves.

Fe Accumulated in the Phloem of *nas4x-2* Plants

The leaf chlorosis phenotype of young *nas4x-2* leaves with green veins and yellow interveinal leaf areas suggests that some residual Fe might be responsible for the greening of veins. We therefore analyzed the localization of Fe in *nas4x-2* leaves of different ages in comparison to wild-type leaves using Perl's Fe stain method. Strikingly, blue Perl's staining was observed in the leaf veins in

(B) and **(C)** *FER1* **(B)** and *YSL1* **(C)** gene expression levels of rosette leaves, determined by quantitative RT-PCR, showing a reduction of gene expression in young leaves and an induction in aged leaves of *nas4x-2* (error bars are SD; $n = 3$; * $P < 0.05$ for the comparison of *nas4x-2* versus the wild type).

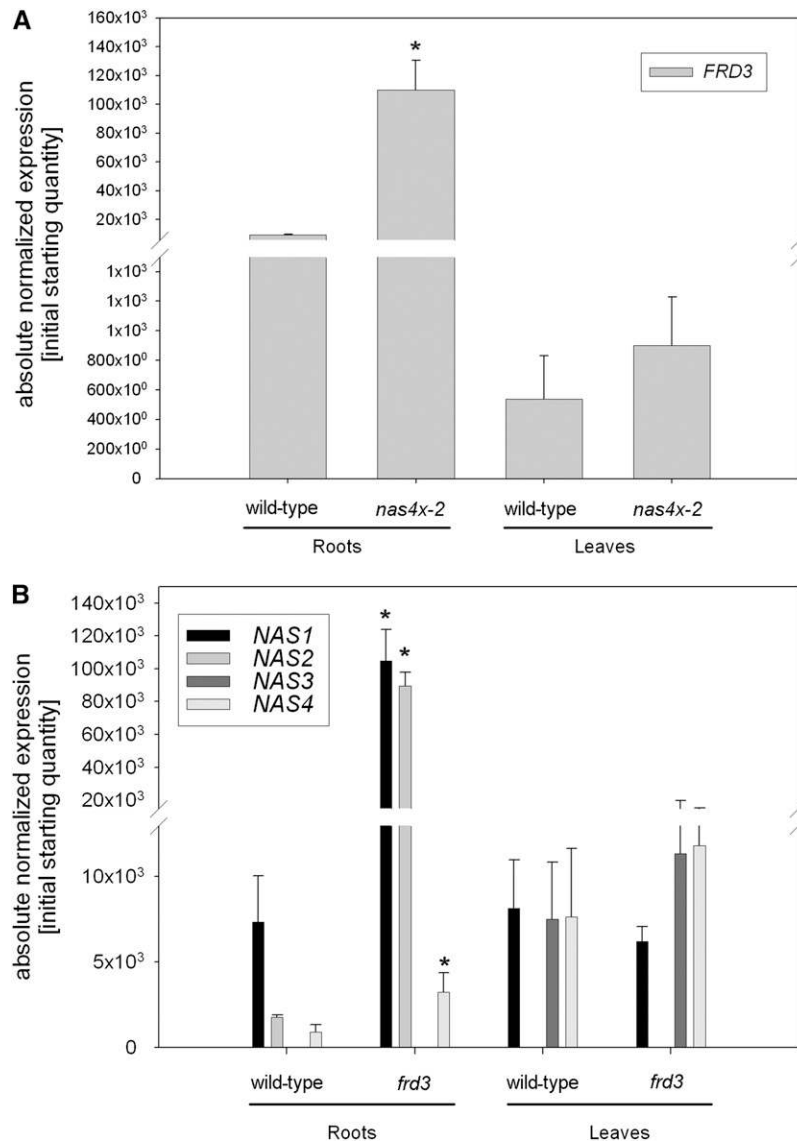


Figure 3. *nas4x-2* and *frd3* Mutant Defects Were Compensated for by the Respective Induction of *FRD3* and *NAS* Genes.

Gene expression levels of *FRD3* (A) and *NAS* (B) genes in the roots and leaves of wild-type, *nas4x-2*, and *frd3* plants, showing an induction of *FRD3* in *nas4x-2* roots and an induction of *NAS1*, *NAS2*, and *NAS4* in *frd3* roots (note that *NAS3* is not expressed in roots). Gene expression was determined by quantitative RT-PCR (error bars are SD; $n = 3$; * $P < 0.05$ for the comparison *nas4x-2* versus the wild type).

young, middle-aged, and aged leaves of *nas4x-2* (Figure 6A; see Supplemental Figure 2 online). It was surprising that this type of Fe accumulation was also observed in the veins of young *nas4x-2* leaves because we had previously found that they were Fe deficient compared with the wild type (Figure 2A). It was also remarkable that Fe accumulation occurred in areas of hydathodes in middle-aged and aged leaves (Figure 6A; see Supplemental Figure 2 online). Hydathodes are known to be connected to the xylem.

Next, we studied Fe deposits in the leaf veins. For this, we generated cross sections from stained *nas4x-2* rosette leaves. We were able to localize Fe in the phloem of young and middle-aged *nas4x-2* leaves, in contrast with the wild type, where no

signals were detected (Figure 6B; see Supplemental Figure 5 online). This result supports the hypothesis that NA is not required for xylem to phloem translocation of Fe but rather for the remobilization of Fe from the phloem. Perhaps translocation of Fe to the phloem and its subsequent mobilization from there is part of a Fe homeostasis network in leaves that serves to distribute Fe to sinks.

Loss of NA Caused Altered Flower Phenotypes and Affected Gene Expression in Carpels and Stamens

Our previous report on *nas4x-1* showed that NA plays a role in seed Fe loading (Klatte et al., 2009). The severe NA-free *nas4x-2*

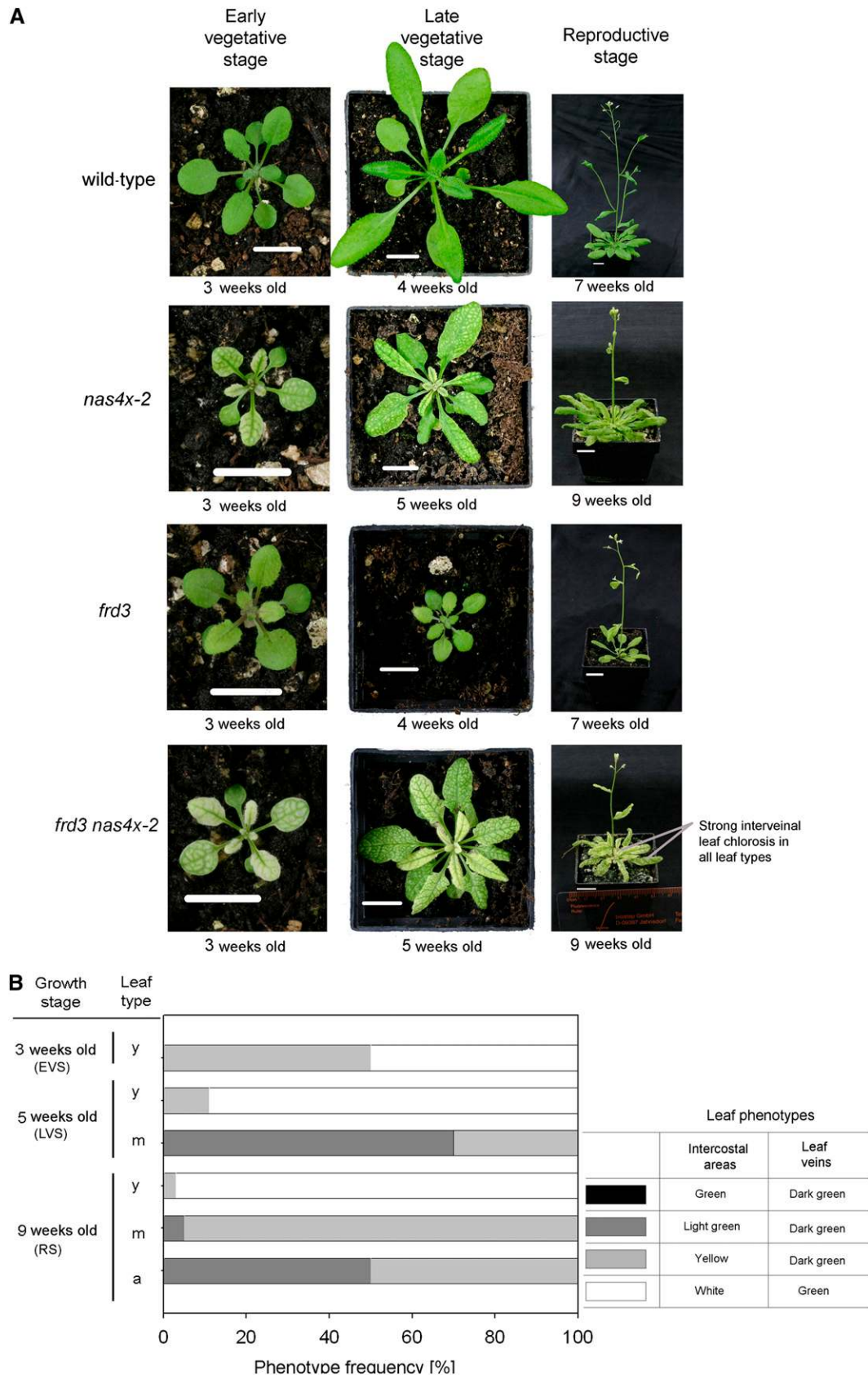


Figure 4. The Double Loss of Function of *FRD3* and *NAS* Epistatic and Synergistic Effects.

mutant does not produce any siliques and seeds and is fully sterile, showing that NA has important functions in plant reproductive biology. In addition, we noted that *nas4x-2* mutants had a late flowering phenotype (see Supplemental Figure 6 online), suggesting that NA was also connected with signaling processes that affect the switch from the vegetative to the RS. *nas4x-2* flowers did not show any strong morphological defects, such as those observed in flowers of the *naat* transgenic tobacco (*Nicotiana tabacum*) lines (Takahashi et al., 2003). Instead, *nas4x-2* flowers exhibited a strongly reduced amount of pollen grains at the anther surface compared with the wild type, indicating that the infertility of *nas4x-2* plants might be linked to the male gametophyte (Figure 7A). Additionally, we observed a slight deformation of *nas4x-2* carpels compared with the wild type, suggesting that the female parts of the flower might also be affected (Figure 7A).

In rescue experiments, we found that the sterility could be reverted by daily application of 5 μ M NA either on leaves or on the inflorescences, supporting the role of NA in reproductive processes. Moreover, silique production was occasionally restored by spraying the inflorescences with 0.05% Fe ethylenediamine-*N,N'*-bis(2-hydroxyphenylacetic acid) (in two out of five plants), indicating that the reproductive defects might be caused by Fe deficiency in the flowers. To investigate the specific role of NA in reproduction, we tested whether *NAS* genes were expressed in the different flower organs. We found that *NAS3* was expressed in the leaf-like floral organs (sepals and petals) but not in the stamen and carpels (see Supplemental Figure 7 online). Other *NAS* genes were not expressed in flowers. We suggest that *NAS3* has a similar function in sepals and petals as in leaves and that NA may serve to mobilize Fe from sepals and petals.

To investigate whether *nas4x-2* flowers were Fe deficient, we determined the Fe contents of *nas4x-2* and wild-type flowers. Flowers of *nas4x-2* plants showed a significant (about twofold) decrease in Fe content compared with wild-type plants (Figure 7B). This observation indicates that NA is needed for translocation of Fe to flowers, as we had previously observed for young leaves.

Next, we tested whether the loss of NA had an effect on Fe homeostasis gene expression in the flower organs by studying the expression of *IRT1*, *FER1*, *YSL1*, *YSL2*, and *YSL3*. We found a striking fourfold induction of *IRT1* in the carpels of *nas4x-2* plants, whereas this gene was hardly expressed in stamens (Figure 7C). This suggests that carpel tissues may rely, at least partially, on Fe mobilization via *IRT1*. We found that *FER1* expression was induced in stamens (about sevenfold) and carpels

(about two to threefold) in *nas4x-2* when compared with the wild type (Figure 7D). *YSL1*, *YSL2*, and *YSL3* were also upregulated in *nas4x-2* carpels and *YSL2* and *YSL3* also in stamens (Figure 7E). These findings support that Fe accumulated in carpels and stamens, presumably in the phloem. This strongly supports a localized accumulation of Fe in *nas4x-2* flower organs, although the total Fe content in flowers was lower in the mutant than in the wild type. Taken together, our data show that the loss of NA affected male and female reproductive organs, presumably due to local Fe precipitation and Fe accumulation in floral organs of *nas4x-2* plants.

***nas4x-2* Plants Were Defective in Male Gametophyte Development**

Next, we examined the effect of the loss of NA in *nas4x-2* homozygous mother plants on male gametophyte development. To determine whether the few *nas4x-2* pollen grains produced by *nas4x-2* mother plants were viable, we used them for pollination of wild-type carpels. We never observed any silique or seed production, indicating that the pollen grains were infertile.

To further clarify this, we investigated the degree of *nas4x-2* pollen germination in vivo using the aniline blue stain. In the wild-type control (wild type \times wild type), pollen germination was visible as the simultaneous elongation of multiple pollen tubes through the pistil toward the ovule (Figure 8A). The pollination of *nas4x-2* pollen onto the wild-type pistil (wild type \times *nas4x-2*) did not yield any pollination tubes (Figure 8A), indicating that *nas4x-2* pollen grains produced by *nas4x-2* mother plants were defective in pollen tube formation. Pollen viability assays using the Alexander staining method showed that the majority of the few produced pollen grains from *nas4x-2* anthers were nonviable (Figure 8B). However, we found that 10 to 15% of these *nas4x-2* pollen grains were able to germinate in vitro (Figure 8C). While 75% of wild-type pollen grains germinated in the absence of Fe and 90% in the presence of 50 μ M Fe sulfate, *nas4x-2* pollen produced by *nas4x-2* mother plants did not show any improvement in in vitro pollen germination after the addition of Fe in this experiment (Figure 8C).

Taken together, the infertility of *nas4x-2* plants can be explained by a reduction of pollen production and by the production of defective pollen that is, to a large extent, nonviable and does not germinate into pollen tubes in vivo. Presumably, the absence of translocation of NA from the *nas4x-2* tapetum cells to the male gametophytes is responsible for this effect.

Figure 4. (continued).

Growth phenotypes of wild-type, *nas4x-2*, *frd3*, and *frd3 nas4x-2* plants grown on soil under long-day conditions up to EVS, LVS, and RS. Note that *nas4x-2* and *frd3 nas4x-2* plants were growth retarded.

(A) Photographs of morphological phenotypes showing that *frd3 nas4x-2* quintuple mutants had a stronger leaf chlorosis than the other mutants. The images for the wild type and *nas4x-2* are reproduced from Figure 1A. Bars = 1 cm.

(B) Comparison of the leaf chlorosis phenotypes of *frd3 nas4x-2* leaves at different growth stages, showing the reduced rescue of leaf chlorosis during maturation of the leaves (cf. to *nas4x-2* in Figure 1C). The different leaf chlorosis phenotypes are described, and the frequency of leaves manifesting these phenotypes is shown.

[See online article for color version of this figure.]

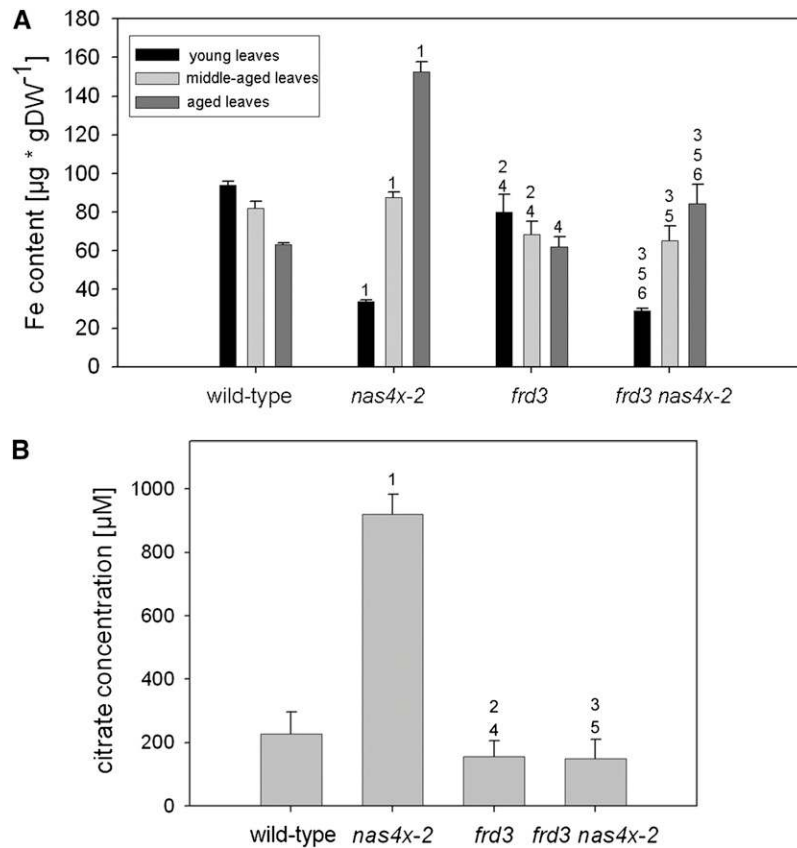


Figure 5. *frd3 nas4x-2* Quintuple Mutants Had a Reduced Fe Content in Leaves and Reduced Concentrations of Citrate in the Xylem.

Plants were analyzed in the RS. Numbers 1 to 6 indicate $P < 0.05$ in the comparisons (1) *nas4x-2* versus the wild type, (2) *frd3* versus the wild type, (3) *frd3 nas4x-2* versus the wild type, (4) *frd3* versus *nas4x-2*, (5) *frd3 nas4x-2* versus *nas4x-2*, and (6) *frd3/nas4x-2* versus *frd3*.

(A) Fe contents of rosette leaves, showing that the elevated Fe content observed in the aged *nas4x-2* leaves was alleviated in *frd3 nas4x-2* ($n = 4$). DW, dry weight.

(B) Concentrations of citrate in the xylem sap, showing that *nas4x-2* plants had an increased citrate concentration compared with the wild type, but not *frd3 nas4x-2* plants ($n = 5$).

NA Was Needed for Pollen Tube Growth through Female Reproductive Tissues

The deformed carpels and high expression levels of Fe homeostasis genes raised the question of whether female reproductive organs of *nas4x-2* mother plants might also suffer from the lack of NA. To test this, we pollinated *nas4x-2* mutant carpels with wild-type pollen (*nas4x-2* \times wild type). Again, we could not find any production of seeds, suggesting a carpel failure. Therefore, we performed a pollen germination assay of this pollination event. We found that wild-type pollen tubes emerged, but then became arrested just above the style of *nas4x-2* plants (Figure 9A). Thus, wild-type pollen tubes were not able to penetrate through *nas4x-2* pistils and pollen tubes did not reach the ovules.

We investigated whether the distribution of Fe was changed in the stylar region of the pistil by performing Perl's Fe staining of unpollinated pistils dissected from closed floral buds. We observed a more intensive blue staining in wild-type pistils than in *nas4x-2* pistils (Figure 9B). This finding is in agreement with the

observed reduction of the total Fe concentration in flowers of *nas4x-2* plants compared with wild-type flowers (Figure 7B). Moreover, the Fe distribution in pistils was altered in *nas4x-2* mutants compared with wild-type plants. Fe accumulation in wild-type pistils was concentrated in small regions distributed along the entire length of the pistils, likely corresponding to the locations of ovules. In *nas4x-2*, we observed blue Fe staining below the stigma, exactly in the area of the style tissue where wild-type pollen tube elongation stopped, but not along the pistil, where ovules were located (Figure 9B). In both the wild type and *nas4x-2*, we noticed Fe accumulation in the stem below the pistil that might represent an area of active Fe transport (Figure 9B). The alteration of Fe distribution in *nas4x-2* further supports the importance of NA for proper Fe distribution in the pistil to permit pollen tube growth toward the ovules.

We analyzed sections of *nas4x-2* pistils to identify structural changes that might explain pollen abortion. Ovaries were developed in *nas4x-2* plants. However, we could detect changes in the formation of the reproductive tract of *nas4x-2* pistils (Figures

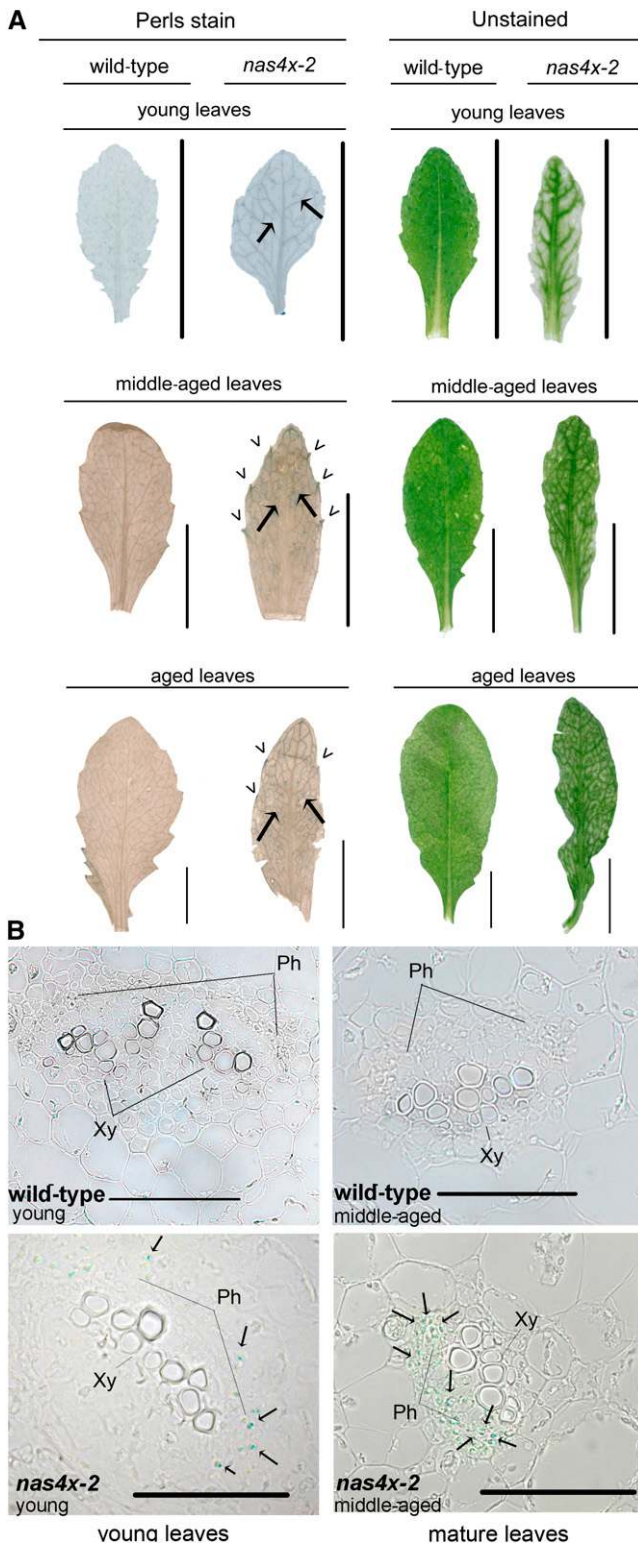


Figure 6. Fe Accumulated in the Vessels and in the Phloem in *nas4x-2* Leaves. Plants were analyzed in the RS. **(A)** Perls Fe staining signals in leaves of the wild type and *nas4x-2*, showing Fe deposits in leaf veins (indicated by arrows) and hydathodes

9C and 9D). The transmitting tract is involved in facilitating pollen tube elongation and has been proposed to have multiple roles in guidance, nutrition, defense, and adhesion (Kim et al., 2004). To facilitate pollen tube migration from the style to the ovary chamber, cells of the transmitting tract undergo developmentally regulated cell death (Crawford and Yanofsky, 2008) (Figure 9C). In our experiment, we were able to observe an opened transmitting tract in wild-type carpels (Figure 9D), whereas the transmitting tract was closed in *nas4x-2* (Figure 9D). The lack of transmitting tract opening may well explain the abortion of pollen tube elongation within the style of *nas4x-2* plants, as was shown by Crawford and Yanofsky (2011).

In summary, we demonstrated that *nas4x-2* sterility was due to several defects, including the production of few and aberrant pollen, defective pollen tube growth, and the failure of carpels to allow pollen tube guidance through the pistil.

nas4x-2 Plants Suffered from Zn Deficiency in Leaves and Flowers

Recently, it was reported that NA is involved in the long-distance translocation of Zn in the metal hyperaccumulating relative of *A. thaliana*, *Arabidopsis halleri* (Deinlein et al., 2012; Haydon et al., 2012). *A. halleri* highly overproduces NA, which is used to transport excess Zn from roots to shoots. Our previous analysis indicated that a reduced NA content correlated with a reduction in Zn content in leaves and flowers of *nas4x-1* plants (Klatte et al., 2009). Therefore, we tested whether the *nas4x-2* plants displayed similar symptoms of Zn deficiency in shoot organs. First, we determined the Zn contents per mass dry weight, and we found that they were lower in rosette leaves, cauline leaves, and senescent leaves of *nas4x-2* than of the wild type (Figure 10A). Furthermore, young and mature leaves of the LVS and RS had increased expression levels of the Zn transporter gene *ZIP4* (Figure 10B). *ZIP4* induction is a marker for Zn deficiency (Grotz et al., 1998). In young leaves of the EVS and in aged leaves of the RS, we did not find any differences in *ZIP4* expression between the mutant and the wild type. The carpels and stamens also showed an induction of *ZIP4* expression (Figure 10C).

Hence, we conclude that due to the lack of NA, the young and mature leaf and flower organs of the LVS and RS were Zn deficient and in consequence induced *ZIP4*. These results confirm that NA is important for long-distance delivery of Zn to leaves and flowers.

Since Zn can be required for pollen function and fertilization, the reproductive failure of *nas4x-2* might be partly due to Zn deficiency. We tested whether Zn supply might affect the germination of pollen in vitro as shown above for Fe. Indeed, we

(marked by arrowheads) of *nas4x-2* leaves; on the right side, unstained control. Further details are available in Supplemental Figure 2 online. Bar = 1 cm.

(B) Perls Fe staining signals in 7- μ m sections of wild-type and *nas4x-2* young and middle-aged leaves, showing Fe deposits in the phloem of the vessels in *nas4x-2* (indicated by arrows); a magnification is shown in Supplemental Figure 5 online. Ph, phloem; Xy, xylem. Bars = 50 μ m.

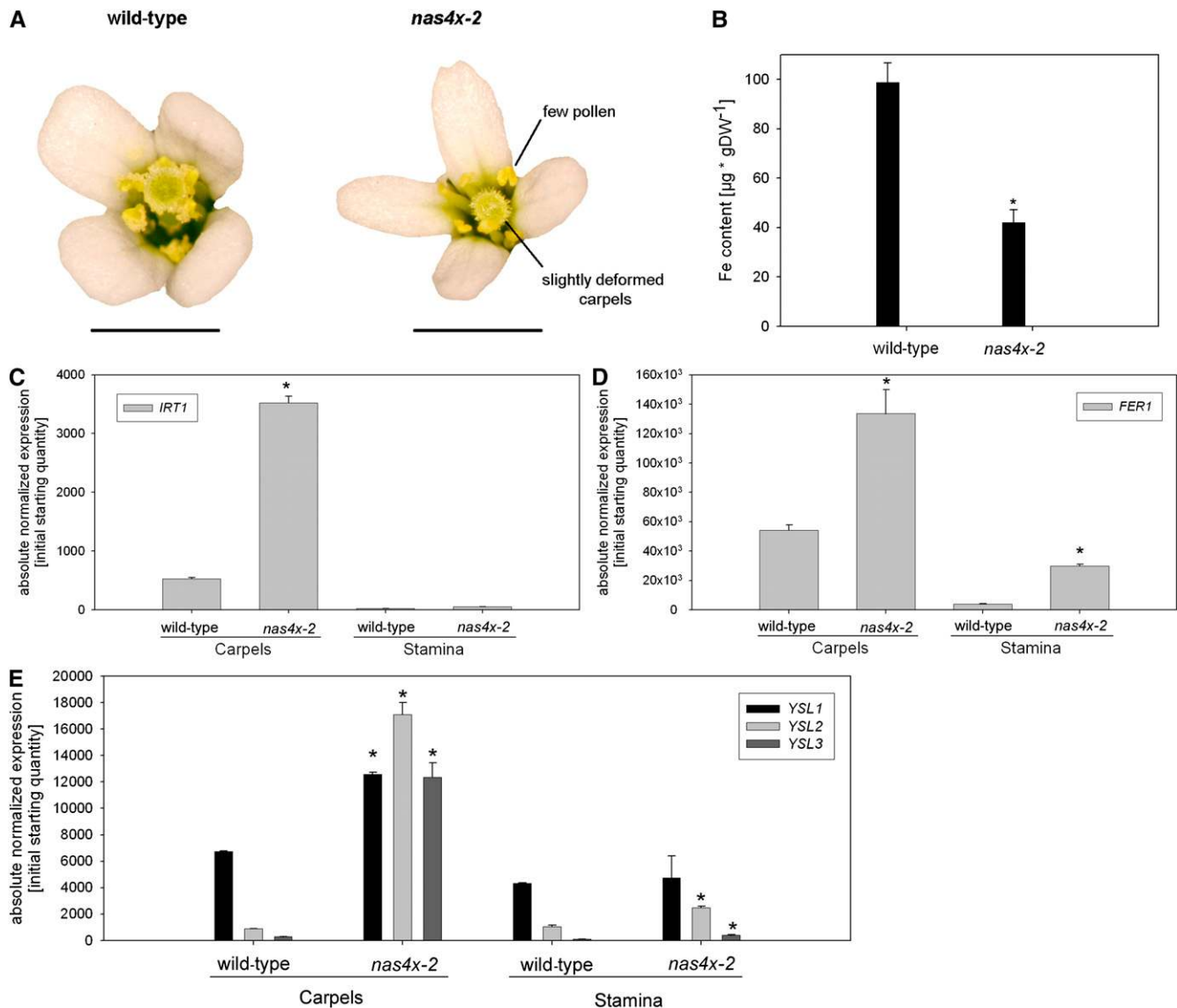


Figure 7. *nas4x-2* Flowers Showed Gene Expression and Morphology Phenotypes in Carpels and Stamens.

(A) Photographs of the morphology phenotypes of *nas4x-2* flowers versus wild-type flowers.

(B) Fe contents of flowers, showing a decrease of total Fe content in *nas4x-2* compared with the wild type (error bars are sd; $n = 4$; * $P < 0.05$). DW, dry weight.

(C) to (E) *IRT1* **(C)**, *FER1* **(D)**, and *YSL1*, *YSL2* and *YSL3* **(E)** gene expression levels in carpels and stamens, showing induction of *IRT1* in carpels and an increase of *FER1*, *YSL2*, and *YSL3* expression in carpels and stamens. Gene expression was determined by quantitative RT-PCR (error bars are sd; $n = 3$; * $P < 0.05$ for the comparison *nas4x-2* versus the wild type).

[See online article for color version of this figure.]

found that a greater percentage of wild-type pollen germinated in the presence of 2 μM Zn sulfate, while no effect of Zn was noted in *nas4-2* pollen germination (Figure 10D). Thus, neither Zn nor Fe supply was able to increase pollen germination in *nas4x-2*. This suggests that the improved in vitro pollen germination efficiency in the presence of Fe and Zn required NA.

Spraying the *nas4x-2* mutants with 0.1% ZnSO_4 did not result in any silique production in five out of five plants (see Supplemental Figure 8 online). However, spraying with both

0.05% Fe ethylenediamine-*N,N'*-bis(2-hydroxyphenylacetic acid) and 0.1% ZnSO_4 successfully restored silique production in four out of five plants (see Supplemental Figure 8 online) and thus was more effective than Fe fertilization alone (restoration in two out of five plants; see Supplemental Figure 8 online). Therefore, a combination of Fe and Zn is required for silique production.

Taken together, the sterility phenotype of *nas4x-2* is caused by a combination of Fe and Zn deficiency in the flowers due to the lack of NA.

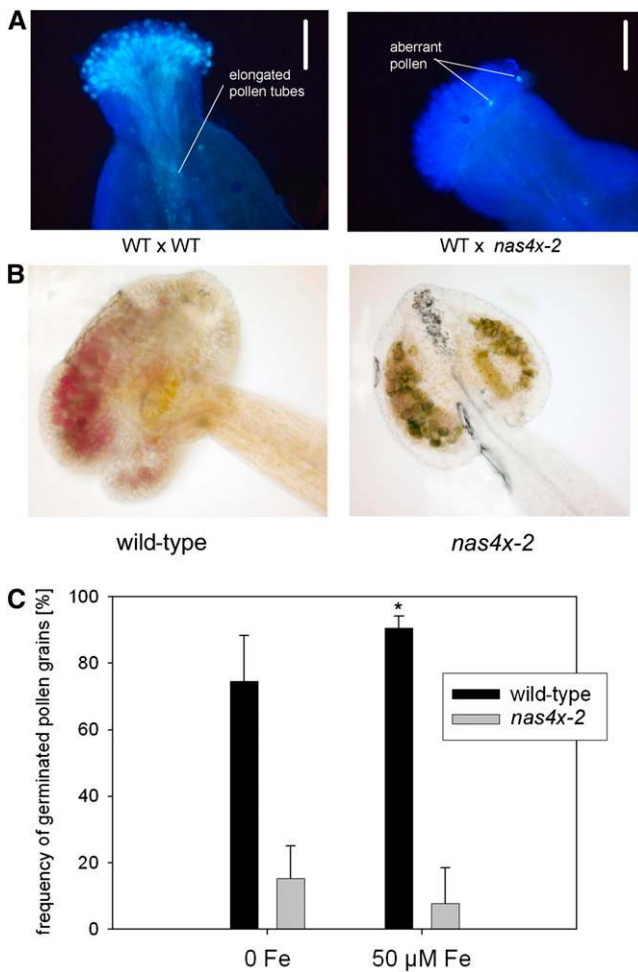


Figure 8. *nas4x-2* Pollen Development and Viability Were Strongly Affected in *nas4x-2* Plants.

(A) In vivo pollen germination after pollination of wild-type (WT) carpels, showing that wild-type pollen produced elongated tubes (wild type \times wild type), while *nas4x-2* pollen was not able to germinate in vivo (wild type \times *nas4x-2*). Pollen germination was visualized by aniline blue staining. Note that only a few pollen grains were produced by *nas4x-2* and that the aberrant *nas4x-2* pollen phenotype was only observed when pollen was produced in fully homozygous *nas4x-2* plants. Bars = 500 μ m. **(B)** Alexander staining of pollen in anthers, showing that *nas4x-2* pollen was mostly nonviable. Viable pollen grains stained dark violet, while nonviable pollen grains were grayish-pale turquoise.

(C) In vitro germination assay of pollen in the absence and presence of 50 μ M Fe sulfate, showing that the frequency of *nas4x-2* pollen germination was strongly reduced and could not be rescued by Fe supply, while wild-type pollen germination was increased in the presence of Fe (error bars are SD; $n = 5$; * $P < 0.05$ for the comparison 50 μ M Fe versus 0 Fe; not indicated $P < 0.05$ for the comparison *nas4x-2* versus the wild type).

DISCUSSION

In this study, we pinpoint the roles of NA in the distribution of Fe and Zn in the plant. We show that NA is involved in the long-distance transport of Fe to sink organs and that it functions in

long-distance transport mainly by mobilization of Fe from the phloem. We demonstrate that NA is essential for pollen development and pollen tube growth. NA is also important for Zn delivery to shoots. The reproductive defect in *nas4x-2* is caused by a combination of Fe and Zn deficiency. Our findings explain the leaf chlorosis and infertility phenotypes of the loss of function NA synthase mutants.

NA Functions in the Translocation of Fe to Sink Organs Involving the Phloem Route

It has been suggested for a long time that NA mediates the long-distance transport of Fe in the phloem. However, the exact function of NA in this process has remained speculative. It was often proposed that NA might be used to unload Fe from the xylem and to reload Fe into the phloem, in particular due to the expression patterns of the potential Fe-NA transporters of the YSL family in the xylem parenchyma (Curie et al., 2009; Palmer and Guerinot, 2009; Conte and Walker, 2011). If this was the case, it would have been expected that in the absence of NA, Fe accumulates in the xylem walls, in the apoplast of the xylem parenchyma, or inside xylem parenchyma cells. This possibility was disproven by our study, which shows that in the absence of NA, Fe was accumulated or trapped in the phloem. Thus, the function of NA is not to facilitate the translocation of Fe into the phloem but to remobilize Fe out of the phloem. This role was found to be particularly important in sink organs. Our findings are explained as follows.

Enhanced long-distance Fe deficiency signaling due to abnormal localization of Fe in *nas4x-2* leaf cells results in increased uptake of Fe into the roots and transport to shoots. We showed that the Fe contents had not generally increased in leaves of *nas4x-2* compared with the wild type. In fact, only middle-aged and aged leaves of the mutants had increased Fe contents compared with the wild type. On the other hand, young leaves of *nas4x-2* had lower Fe contents than the wild type and were associated with a much stronger leaf chlorosis than observed in middle-aged and aged leaves. Thus, young leaves must depend on NA for Fe acquisition, which explains the stronger phenotypes of the young *nas4x-2* leaves. Similarly, flowers of the mutant were Fe deficient compared with those of the wild type, and their sterility supports the functional lack of Fe (and Zn). Especially during the development of leaves, flowers, and seeds, these young organs act as sinks, and the requirement for phloem transport of micronutrients to these sinks is high. A recent study provided evidence that young leaves of barley (*Hordeum vulgare*) receive Fe primarily from the phloem, while older leaves receive Fe from the xylem (Tsukamoto et al., 2009). The conclusion that sink organs rely on a NA-dependent phloem pathway for obtaining adequate levels of Fe is supported by our finding that Fe accumulated in the phloem in the absence of NA. In *nas4x-2* plants, Fe was not mobilized from the phloem. The transport of Fe into the phloem presumably only occurred in leaf cells, since it was preceded by the xylem-based transport of Fe mediated by citrate. *frd3* mutants have a 40% reduced citrate content in the xylem (Rogers and Guerinot, 2002; Green and Rogers, 2004). Double *frd3 nas4x-2* mutant plants were therefore an optimal tool to study the long-distance transport of Fe to

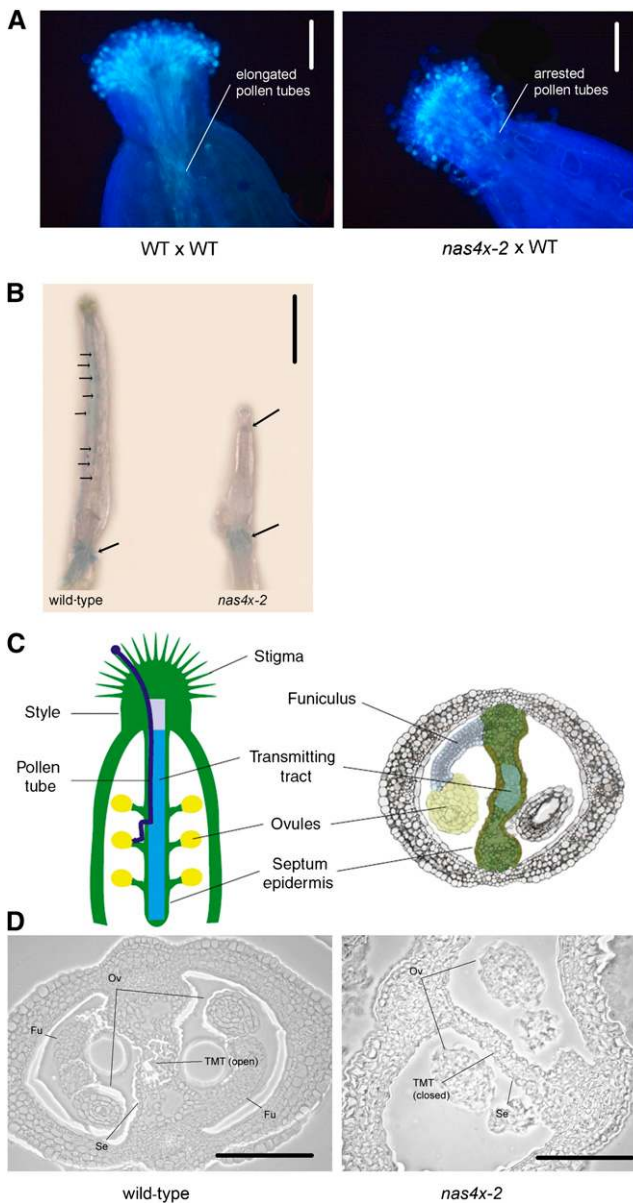


Figure 9. Pollen Tube Growth Was Arrested in *nas4x-2* Carpels.

(A) In vivo pollen germination, showing that wild-type (WT) pollen produced elongated tubes that were arrested below the style in *nas4x-2* carpels (*nas4x-2* × wild type), in contrast with the controls (wild type × wild type). Pollen germination was visualized by aniline blue staining. Bars = 500 μ m. **(B)** Perls Fe staining, showing that Fe accumulated at the sites of the ovules and at the bottom of the ovary in the wild type, while Fe accumulation was visible at the bottom of the style and at the bottom of the ovary in *nas4x-2* (Fe staining indicated by arrows). Bar = 1 mm. **(C)** Illustration of longitudinal (left) and transverse (right) *A. thaliana* carpel sections. Note the position of the transmitting tract, which opens due to induced cell death in mature carpels. (Figure reproduced from Crawford and Yanofsky [2008].) **(D)** Transverse sections of wild-type and *nas4x-2* ovaries showing that the transmitting tract of the ovary was closed in *nas4x-2*, while it was open in the wild type. Fu, funiculus; Ov, ovule; Se, septum epidermis; TMT, transmitting tract. Bars = 125 μ m.

leaves in *nas4x-2*. The study of the quintuple *frd3 nas4x-2* mutant demonstrated that the high Fe accumulation in aged *nas4x-2* mutant leaves did not occur in *frd3 nas4x-2* and that the leaves were highly chlorotic in this quintuple mutant. This showed that citrate was responsible for the transport of the excessive Fe to aged leaves of *nas4x-2*. The severe leaf chlorosis of *frd3 nas4x-2* mutants must therefore be the consequence of defective long-distance Fe transport. Hence, the accumulation of Fe in the phloem in *nas4x-2* leaves required the action of the citrate transporter FRD3 in the roots. An additional indication that NA was not involved in mediating long-distance transport of Fe was found recently by studying overexpression of the NA nbsp; transporter ZINC-INDUCED FACILITATOR1 (ZIF1) (Haydon et al., 2012). ZIF1 overexpression resulted in increased sequestration of NA inside the vacuoles of root cells. Consequently, the plants developed Zn deficiency and Fe overaccumulation in the shoot. This phenotype conferred by ZIF1 overexpression was similar to the *nas4x-1* and *nas4x-2* mutant phenotypes. Thus, trapping of NA in root vacuoles or loss of function of NA production both result, on one side, in reduced transport of Zn to leaves, and on the other side in Fe deficiency of sinks and an alteration in the long-distance signaling of Fe to roots (as phloem Fe mobilization is defective).

To summarize and explain our findings, we suggest the following model: First, Fe is taken up into the roots and reaches the root stele. This process occurs in the absence of NA and therefore does not require NA as deduced from the observation that Fe accumulated in the root stele in *frd3 nas4x-2* quintuple mutants. Next, the directional transport of Fe from roots to leaves takes place in the xylem using the transpiration stream. The xylem-based transport requires citrate. *frd3* mutant plants with a reduced concentration of citrate in their xylem accumulate Fe in the root stele, since the transport of citrate into the xylem is hampered. However, the middle-aged and aged leaves of the *nas4x-2* mutant contain high levels of Fe, indicating that in the absence of NA, Fe was able to reach these leaves. Since the quintuple *frd3 nas4x-2* mutant did not exhibit high Fe levels in its aged leaves, it can be concluded that the accumulation of Fe in aged *nas4x-2* leaves depended on the transport of Fe citrate in the xylem. Based on YSL expression patterns, it was proposed that Fe-NA is transported from the xylem across the xylem parenchyma to the adjacent leaf tissues using YSL1, YSL2, or YSL3 transport proteins (Conte and Walker, 2011). However, we found that this suggested lateral transport route for Fe from xylem to leaf parenchyma seemed to occur also in the absence of NA in aged leaves. We therefore propose that lateral transport may rely on citrate and FRD3 rather than on NA. Citrate is used to mobilize extracellular Fe from the apoplast throughout plant development, and this could also be important during lateral transport of Fe from the xylem to the leaf parenchyma (Roschztardt et al., 2011). This is supported by the finding that *frd3 nas4x-2* leaves are strongly chlorotic and do not recover from the chlorosis with age, in contrast with *nas4x-2*. Finally, for transport of Fe to young sink leaves, Fe is translocated from the xylem to the phloem. Due to the observation that a functional FRD3 gene was needed for translocation of Fe into the phloem in *nas4x-2* leaves, we deduce that the translocation took place in the leaves after Fe was transported upwards in the xylem. The

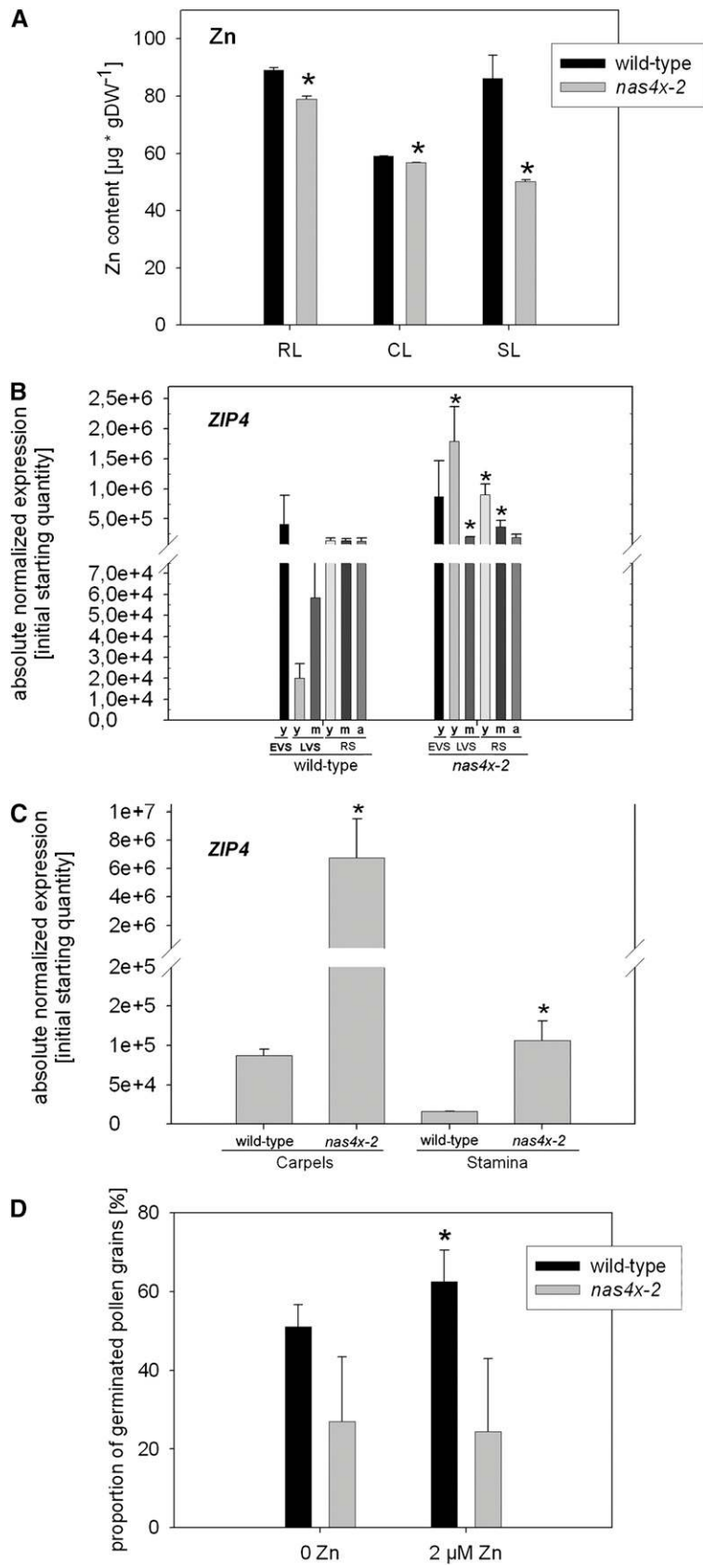


Figure 10. *nas4x-2* Plants Were Zn Deficient.

xylem-to-phloem translocation was not dependent on NA, since *nas4x-2* leaves accumulated Fe in the phloem. Hence, it seems that NA is required for the lateral movement of Fe from the phloem to surrounding tissues in young leaves, while this function is replaced by citrate in aged leaves. Fe deficiency could furthermore act as a signal that triggers the activation of the translocation of Fe into the phloem to nourish sink organs under Fe deficiency. This would explain the presence of high Fe in the phloem in *nas4x-2* mutants, which show signs of Fe deficiency (Klatte et al., 2009; Schuler et al., 2011). Presumably, the phloem pathway is needed in young organs because the differentiation of xylem is slower than that of phloem, or the xylem-dependent Fe transport pathways are neglected in young leaves because of insufficient transpiration.

The question arises as to which type of transporters mediates the transport of Fe into and out of the phloem. Translocation of Fe out of the xylem and into the phloem occurs irrespective of NA and therefore does not seem to involve Fe-NA transporters, as mentioned above. It was reported that citrate also chelates Fe in the apoplast of leaf cells (Roschztardtz et al., 2011), and this complex may facilitate the transport of Fe out of the xylem into adjacent cells. Ferric reductase genes and divalent metal transport genes are expressed in leaves (Guerinot, 2000; Mukherjee et al., 2006). Therefore, it is possible that reduced Fe is transported into the phloem. Further studies are needed to determine the identity of the phloem import components. From the elevated pH of the phloem, it is unlikely that Fe is reduced inside the phloem and exported as a divalent ion. Moreover, the phloem sap contains Fe binding proteins like IRON-TRANSPORT PROTEIN (Kruger et al., 2002). Hence, it makes sense that an effective chelator binds Fe and transports it out of the phloem, and our study suggests that this chelator is NA. YSL proteins may act as Fe-NA transporters. YSL1 and YSL2 transporters seem to be active mainly in the xylem parenchyma of the leaf veins but not the phloem cells themselves (DiDonato et al., 2004; Le Jean et al., 2005; Schaaf et al., 2005; Waters et al., 2006). YSL3 promoter activity was detected throughout the parenchyma of veins but not in xylem or phloem (Waters et al., 2006). However, more YSL genes are present in the genome, and their functional analysis has not been completed (Curie et al., 2009). Other small peptide transporters may also fulfill the function of a Fe-NA transporter, such as OLIGO-PEPTIDE TRANSPORT3 (OPT3) protein. OPT3 expression was

detected in the vasculature (Stacey et al., 2008). *opt3* mutants overaccumulate Fe and other metals in rosette leaves and in sink organs except seeds. Thus, OPT3 could be involved in Fe phloem loading and in postphloem transport (Stacey et al., 2008). Our results speak against the possibility that OPT3 transports Fe-NA into the phloem, but still it might translocate other organic compounds bound to Fe. It is possible that OPT3 transports Fe-NA out of the phloem, so that *opt3* mutants turn similarly Fe deficient and overaccumulate Fe as *nas4x-2*. Further research will help to refine Fe-NA transport in leaves and OPT3 function.

The molecular-physiological study of the quintuple *frd3 nas4x-2* mutant demonstrated a synergistic interaction between *FRD3* and *NAS*. Previously, it was reported that NA was increased in *frd3* mutants and that induction of *FRD3* took place in *nas4x-1* roots compared with wild-type roots under Fe supply conditions (Rogers and Guerinot, 2002; Schuler et al., 2011). We could provide further support that indeed NA and citrate might compensate the loss of each other. We found that *NAS* genes were induced in *frd3* mutants and that *FRD3* was induced in *nas4x-2*. Furthermore, the xylem citrate concentration was increased in the *nas4x-2* mutant. These facts highlight the crosstalk in the plant that must exist to comply with the needs for Fe. In *frd3* mutants, Fe accumulates in the roots, irrespective of NA, as we could demonstrate here. However, this accumulation of Fe is not likely the trigger for the induction of *NAS* genes in the root. Several of the root-expressed *NAS* genes are induced by Fe deficiency signals in roots and are part of the Fe deficiency response that serves to increase Fe acquisition (Bauer et al., 2004). The upregulation of *NAS* genes by Fe deficiency and in the roots of *frd3* mutants indicates that under Fe deficiency and in the absence of a functional Fe-citrate transport, NA is used as an alternative to enhance the transport of Fe, presumably in the phloem. We therefore enlarge our model and propose that the actual long-distance transport of Fe-NA in the phloem may be relevant upon Fe deficiency in *A. thaliana* when the Fe-citrate transport is low, but not under normal Fe supply. Additional carboxylates might also be involved in long-distance Fe transport. However, this aspect requires further investigation since none of the additional putative organic acid ligands tested by us (malic acid, succinic acid, and 2-oxoglutaric acid) was significantly increased in the quintuple mutant xylem sap.

Figure 10. (continued).

- (A)** Zn contents of rosette (RL), cauline (CL), and senescent (SL) leaves of plants grown to the RS, showing that Zn contents were reduced in leaves of *nas4x-2* plants (error bars are SD; $n = 4$; * $P < 0.05$ for the comparison *nas4x-2* versus the wild type). DW, dry weight.
- (B)** *ZIP4* expression levels in leaves of different growth stages, determined by quantitative RT-PCR, showing an induction of gene expression in leaves of *nas4x-2* (error bars are SD; $n = 3$; * $P < 0.05$ for the comparison *nas4x-2* versus the wild type). Plants were grown on soil under long-day conditions up to the EVS, LVS, and RS; young (y), middle-aged (m), and aged (a) rosette leaves were harvested for analysis (see phenotypes in Figure 1).
- (C)** *ZIP4* expression levels in carpels and stamen, showing induction of *ZIP4*. Gene expression was determined by quantitative RT-PCR (error bars are SD; $n = 3$; * $P < 0.05$ for the comparison *nas4x-2* versus the wild type).
- (D)** In vitro germination assay of pollen in the absence and presence of 2 μM Zn sulfate, showing that the frequency of *nas4x-2* pollen germination was strongly reduced and could not be rescued by Zn supply, while wild-type pollen germination was increased in the presence of Zn (error bars are SD; $n = 5$; * $P < 0.05$ for the comparison 2 μM Zn versus 0 Zn; not indicated $P < 0.05$ for the comparison *nas4x-2* versus the wild type).

Taken together, we favor the model that in the presence of citrate and sufficient Fe in the root, NA is not required for the actual long-distance transport from root to shoot in *A. thaliana* plants. However, under Fe deficiency, when Fe-citrate is low, NA may be recruited to assist in long-distance Fe transport involving the phloem. Generally, NA is needed for the unloading process and remobilization of Fe from the phloem in *A. thaliana*, which is especially important in the sink organs. In graminaceous species like barley, the situation might be different, and NA and phytosiderophores might be more generally involved in long-distance transport (Tsukamoto et al., 2009; Nishiyama et al., 2012).

Successful Reproduction Requires NA for Pollen Development in the Anthers and for Pollen Tube Growth in the Female Pistil Tissue

Although we have known for a long time from studies of tomato (*Solanum lycopersicum*) and tobacco NA mutants that NA is needed for reproduction (Scholz et al., 1992; Takahashi et al., 2003), this phenomenon was until now not further explained, and experiments as to which process of reproduction is hampered had not been performed. Using reciprocal crosses, pollen viability tests, and pollen in vitro and in vivo germination tests as well as anatomical analysis, we can show that the processes affected are pollen development and viability as well as pollen germination and pollen tube passage in the carpel. In *nas4x-2* carpels, we could find no indication of transmitting tract opening. We were able to rescue the infertility by exogenous application of NA, which supports the fundamental role of NA in these reproductive processes. In addition, we found that fertilizing the plants with both Fe and Zn was able to restore *nas4x-2* silique growth. Therefore, both Fe-NA and Zn-NA are needed for reproduction.

While tobacco NA-free mutants have deformed flower morphology phenotypes (Takahashi et al., 2003), we found here that *A. thaliana* flowers appear almost normal in their morphology with only slightly deformed carpels. The phenotypes of *A. thaliana* NA-free plants are connected with pollen production, viability, and germination, since all three processes were dramatically reduced in the mutant *nas4x-2* flowers. These *nas4x-2* pollen phenotypes were apparent only when mother plants were homozygous NA-free plants but not when mother plants were heterozygous and produced residual amounts of NA. Hence, NA produced by the mother plant is important for pollen functioning, while the male gametophyte itself does not need to produce any NA. Most probably, the male gametophytes depend on NA produced by the mother tissues to meet their requirement for Fe and Zn. NA could be involved again in mobilizing Fe out of the phloem in the anthers. In addition, it could act in transporting metal-NA complexes across the tapetum cells to the microspore cells and developing pollen grains. Other divalent Fe transport mechanisms might not function in an adequate manner. It has been described earlier that the *IRT1* promoter was induced by Fe deficiency in anthers (Vert et al., 2002); however, we did not note any induction of *IRT1* in *nas4x-2* anthers, only in carpels. Therefore, activation of *IRT1* for acquisition of reduced Fe did not compensate for the loss of NA in anthers. The metals

translocated by NA are needed during meiosis, pollen development, and sporopollenin wall fortification as well as for pollen viability. As we demonstrated here, Fe and Zn supply enhance pollen germination. A lack of adequate metal supply would therefore explain the observed pollen phenotypes of *nas4x-2*.

Our results are in line with previous reports on the function of YSL1 and YSL3. If Fe-NA is a substrate for YSL1 and YSL3, it is expected that these transport proteins together with NA are involved in the same biological process. *YSL1* is active during pollen production in anthers and in ovules (Le Jean et al., 2005; Waters et al., 2006), and *YSL3* is active in anthers and in pollen (Waters et al., 2006). The double *ysl1 ysl3* mutants have pollen defects and are partially sterile, which could be reverted by Fe fertilization (Waters et al., 2006). Thus, YSL1 and YSL3 are required for reproduction, and the double loss of function mutants have similar phenotypes as *nas4x-2*. These observations strongly point to a joint action of the YSL proteins and NA, suggesting that YSL1 and YSL3 may indeed transport metal-NA complexes during reproduction. Recently, it was deduced from grafting studies that, although YSL1 and YSL3 affect reproductive processes, their functions seem sufficient in the vegetative leaves (Chu et al., 2010). Inflorescence grafting of *ysl1 ysl3* onto the wild type rescued pollen and seed production. The authors speculated that YSL1 and YSL3 are important for retranslocation of Fe from source leaves to sinks. Nevertheless, the grafted *ysl1 ysl3* shoots had lower metal contents in their seeds than the wild-type grafts, indicating that the two proteins are involved in metal supply during seed production in the inflorescence. The phenotype of *nas4x-2* plants is more severe than that of *ysl1 ysl3* plants, probably because NA is essential, while the function of YSL1 and YSL3 can be replaced by the function of alternative metal-NA transport proteins of the YSL or other families.

Interestingly, the reduced pollen functionality was not restored when the few developed mutant pollen grains were used to pollinate wild-type carpels. Hence, a translocation of NA from carpel tissue to the pollen grains, prior or upon pollen germination, did not seem to take place or at least could not rescue the phenotype. On the other hand, we found that NA was also required at a later step of pollination, namely, pollen tube growth. At this stage, NA was needed in the female carpel tissue of the style to allow the passage of pollen tubes toward the ovules. Even wild-type pollen became arrested in the style of *nas4x-2* pistils, indicating that NA present in the wild-type pollen was not translocated to the surrounding female tissue to rescue the *nas4x-2* phenotype. We detected an accumulation of Fe in *nas4x-2* carpels exactly in the area of the styles where pollen tubes were arrested. Furthermore, *FER1* was induced in carpels of *nas4x-2* compared with the wild type. Carpels also showed an upregulation of the Fe deficiency marker *IRT1* as well as of *YSL2* and *YSL3*. We found that Fe accumulated at the base and in the stylar region of the *nas4x-2* carpels, while it was lacking in the places of ovules along the ovary. Hence, it seems that *nas4x-2* carpels locally accumulated Fe, resulting in local Fe sufficiency, while locations of Fe deficiency were also present due to reduced mobilization of Fe from the phloem caused by the lack of NA.

A clue to the function of NA in the female pistil tissue of the style came from the finding that *nas4x-2* plants failed to form the transmitting tract in this region. The style connects the stigma to the ovary chambers, and in *A. thaliana*, it is short and closed at first (Crawford and Yanofsky, 2008). Then, the central cells of the connective tissue between the two ovary chambers degenerate such that an opening occurs. This transmitting tract facilitates pollen tube movement and has been proposed to have multiple roles in guidance, nutrition, defense, and adhesion (Kim et al., 2004; Crawford and Yanofsky, 2008). Recent studies in *A. thaliana* have shown that controlled degeneration and death of these transmitting-tract cells are important for pollen tube movement (Crawford et al., 2007; Crawford and Yanofsky, 2011). One explanation for the failure of transmitting tract formation in *nas4x-2* plants might be that Fe is needed to induce programmed cell death. An alternative explanation for pollen tube abortion in *nas4x-2* carpels is that, in *A. thaliana*, germinating pollen tubes may be sustained by energy sources and high mitochondrial activity, which require Fe-NA (Rounds et al., 2010). Many other plant species may not require Fe uptake during pollen tube formation, since pollen tubes are also able to grow in vitro on a matrix in the absence of micronutrients (Fan et al., 2001) and pollen tubes of some species germinate in water alone (Johri and Vasil, 1961). Interestingly, we found that the germination of *A. thaliana* wild-type pollen was enhanced in vitro in the presence of Fe or Zn, suggesting that the pollen grains could take up Fe and Zn in vitro. *nas4x-2* pollen germination was not enhanced by the application of Fe or Zn in vitro. In our in planta experiments, the self-pollination of *nas4x-2* was partially rescued by Fe but not by Zn fertilizer, whereas it was rescued by the application of NA or a combination of Fe and Zn fertilizer. Perhaps NA is needed in *A. thaliana* to mobilize Fe and Zn within the mother carpel tissues to transport Fe and Zn toward growing pollen tubes.

Due to these severe early defects caused by the lack of NA in pollen and in the upper carpel style region, we were not able to unravel the later potential roles of NA in female gametophyte function, in fertilization, and in embryo and seed development. We observed that ovules were formed in *nas4x-2* carpels, suggesting that development of female gametophytes took place.

Conclusion

The *nas4x-2* mutant was proven to be an optimal tool to study the functions and sites of action of NA in Fe and Zn homeostasis.

We provided novel evidence that NA is required for Fe mobilization in the phloem, for root-to-shoot transport of Zn, and, during reproduction, for nutrition of the male gametophyte with Fe and Zn and for passage of pollen tubes in the style. An understanding of the mechanisms by which Fe and Zn are delivered via NA to sink organs will provide new opportunities to efficiently manipulate Fe and Zn homeostasis in plants. Optimal growth and fertilization is the basis for obtaining grain products with increased Fe and Zn content and optimal bioavailability of these metal ions. From our studies, we suggest that Fe transport to seeds could be optimized if NA is produced in the phloem-associated cells of leaves and flowers, while optimal Zn supply

might be achieved through the additional production of NA in the proximity of the root xylem. Knowledge about the sites of NA production and the sites of its effect as well as of the functions in planta will help to refine biofortification strategies.

METHODS

Plant Material

The *Arabidopsis thaliana* ecotype Columbia-0 was used as the wild-type control. *nas4x-2* was described (Klatte et al., 2009). *frd3 nas4x-2* mutants were obtained by crossing a homozygous *frd3-3* plant (from the Nottingham Arabidopsis Stock Centre) with a triple homozygous *nas1-1 nas2-2 nas3-1* heterozygous *nas4-1* plant. The resulting F1 plants were selfed, and in the F3 generation, a homozygous line of *frd3-1 nas2-2 nas3-1 nas4-1* segregating for *nas1-1* was selected and used to obtain homozygous quintuple *frd3 nas4x-2* plants. During the generation of this quintuple mutant line, *nas* genotypes were verified by PCR (Klatte et al., 2009), and the *frd3* genotype was selected based on Perls Fe staining of the roots (Green and Rogers, 2004). Homozygous quintuple *frd3 nas4x-2* mutant plants were identified by their strong leaf chlorosis, and the genotype of *nas1-1/nas1-1* was confirmed by PCR genotyping. Only homozygous quintuple mutant plants with *nas1-1/nas1-1* were used in the physiological experiments.

Plant Growth

Seeds were surface-sterilized and stratified for 2 to 3 d at 4°C. *A. thaliana* plants grown on soil were placed on a turf substrate mixed 3:1 with vermiculite. Hydroponic growth was described by Klatte et al. (2009). Briefly, seedlings were germinated on quarter-strength Hoagland agar medium in 500- μ L support tubes. After 2 weeks, plants were placed into quarter-strength Hoagland liquid medium for another 2 weeks. Medium was exchanged weekly. The regular control medium contained 10 μ M Fe(III)-EDTA and is described by Klatte et al. (2009). Solid germination medium of the hydroponic system contained no Suc and 0.6% plant agar. Four weeks after germination, plants were exposed for 1 week to plant medium containing either 10 μ M Fe(III)-EDTA (+Fe) or no Fe (-Fe). Cultivation took place at 21°C/19°C, with 16-h-light/8-h-dark cycles, a light intensity of 150 μ mol m⁻² s⁻¹, and a humidity of 60% in plant chambers of CLF Plant Climatics.

Plant Morphological Analysis and Analysis of Plant Sections

Wild-type and *frd3* plants were analyzed after 3 weeks in their EVS, after 4 weeks in their LVS, and after 7 weeks in their RS. Plants with the *nas4x-2* background were retarded in their development. Therefore, the EVS was investigated after 3 weeks, the LVS after 5 weeks, and the RS after 9 weeks. The following leaf chlorosis phenotypes were distinguished: Strong leaf chlorosis was characterized by white intercostal areas with green leaf veins. Normal leaf chlorosis was manifested as yellow intercostal areas with dark-green veins, while light leaf chlorosis was categorized as light-green intercostal areas. Very weak leaf chlorosis was observed as green intercostal areas with dark-green veins. Young leaves were expanding leaves, while medium-aged leaves were fully expanded. Aged leaves were fully expanded and just entering the senescence phase. For analysis of sections, plant organs were dissected and fixed with methacarn (methanol/chloroform/pure acetic acid, 6:3:1) at room temperature. Fixative was removed and plant organs were washed three times with distilled water and dehydrated in successive baths of 10, 30, 50, 70, 90, 95, and 100% ethanol, butanol:ethanol (1:1), and 100% butanol. Then, the plant organs were embedded in the Technovit 7100 resin (Heraeus-Kulzer) according to the manufacturer's instructions, and thin

sections (7 μm) were obtained using a rotation microtome. Sections were analyzed and photographed using the BZ-8100 microscope from Keyence.

Gene Expression Analysis

Gene expression analysis was performed by quantitative real-time RT-PCR as previously described (Wang et al., 2007; Klatte and Bauer, 2009; Klatte et al., 2009). Briefly, DNase-treated RNA was used for cDNA synthesis. SYBR green I-based real-time PCR analysis was performed using TaKaRa Premix in the real-time ICycler (Bio-Rad). For each gene, the absolute quantity of initial transcript was determined by standard curve analysis using mass standards. Absolute expression data were normalized against the averaged expression values of the internal control genes *EF1B α 2* and *UBP6* (Klatte and Bauer, 2009). Each biological cDNA sample was tested in two technical replicates and the values averaged. Statistical analysis by *t* test was performed using the values of two to three biological replicates derived from different plants, as indicated in the figure legends. *NAS*, *IRT1*, *FRO2*, *FER1*, and *YSL* oligonucleotide primer sequences are described (Klatte et al., 2009). Sequences of *FRD3* 5' and 3' reverse transcription PCR primers used are 5'-ATGGCCATCGGAATACCGTT-3' and 5'-CTAGGAAGATGAAGAGGATGATCGT-3'. Sequences of primers used to generate *FRD3* mass standards are 5'-GCATCTTTCGTGGATTCAAGGA-3' and 5'-AAGGAAGAAGAGATGCAACTCGTT-3'. Sequences of *ZIP4* 5' and 3' RT-PCR primers used are 5'-TGGTTGGGGAAAGAGTGACCGATAA-3' and 5'-TACCCCCAGGGA TAAACCGATGATG-3'. Sequences of primers used to generate *ZIP4* mass standards are 5'-TTTTGCAGATCATTCCCGAGACAAT-3' and 5'-AGCTGCAATAAGAGGCTGATCGT-3'.

Fe and Zn Measurements

For metal determination, roots were washed with 100 mM $\text{Ca}(\text{NO}_3)_2$ prior to harvest to eliminate metal residues from the growth medium. Plant material was dried overnight at room temperature and then for 1 d at 120°C and powdered with an achat mortar. Quantification of metal contents of the plant samples was performed using an atomic absorption spectroscopy 6 Vario instrument from Analytik Jena equipped with a transversely heated graphite tube atomizer, an automatic solid sampling accessory SSA 61 (including a Sartorius M2P microbalance with a precision of 1 μg), and continuum source background correction. Calibration curves of aqueous reference standards with appropriate concentrations were obtained by wide-range determination of the absorbance from five different standard volumes (0, 5, 8, 11, and 14 μL). Four technical replicate measurements were performed with weighted samples of 50 to 120 μg for every atomization (2300°C), and mean mass per dry weight values were calculated for each biological sample. Four biological replicates were produced, mean values calculated, and statistical *t* tests performed, as indicated in the figure legends.

Collection and Analysis of Xylem Sap

Xylem sap was collected from plants in the RS. To increase root pressure for the collection of xylem sap, the relative air humidity was increased by covering soil-grown plants with a dome 2 d before xylem sap collection. Xylem sap was collected by excision of the hypocotyls below the rosette with a sharp scalpel. The first droplet was discarded to minimize possible contamination. Then, a pipette tip was carefully mounted over the stem and xylem sap was subsequently soaked into the mounted pipette tip due to capillary forces. Sap was collected over a period of 30 min in a pipette tip. Care was taken not to extend the collection time beyond 30 min, since this could have affected xylem composition. Xylem exudates were pooled from five to seven plants for one biological replicate. The total volume was determined and the samples were stored at -80°C . Determination of

organic acid concentration was performed using HPLC–electrospray ionization–time-of-flight–mass spectrometry as described (Rellán-Alvarez et al., 2011). Mean concentrations of biological replicates were calculated and statistical analysis performed using a *t* test.

Perls Fe Stain Method

The Perls Fe stain method was previously described (Green and Rogers, 2004; Roschztardt et al., 2011). Leaves and flowers were harvested freshly and were vacuum infiltrated with the fixative methacarn (methanol/chloroform/pure acetic acid, 6:3:1) and incubated for 1 h at room temperature. Fixative was removed and plant organs were washed three times with distilled water and subsequently vacuum infiltrated with equal volumes of Perls stain solution (4% HCl and 4% K-ferrocyanide, 1:1) for 15 min to 5 h at room temperature. The reaction was stopped by washing three times with distilled water. Plant organs were either analyzed immediately or embedded in Technovit and sectioned as detailed above.

Pollen Viability Stain and Germination Assay

Pollen viability was tested using the Alexander stain. For this assay, anthers were removed and placed for 2 h at 50°C into a solution containing water and organic solvents, malachite green, acid fuchsin, and orange G as described (Johnson-Brousseau and McCormick, 2004). Pollen grains that were viable stained dark blue or purple, while dead pollen grains stained pale turquoise blue. For in vivo pollen germination, pistils were collected 24 h after controlled pollination and fixed in a solution containing 70% ethanol, 3.7% formaldehyde, and 10% acetic acid for 24 h. The fixed material was then briefly washed and incubated for 24 h in 10 M NaOH and for another 24 h in aniline blue solution (0.1% aniline blue in 0.1 M K_3PO_4 , pH 7.0). Pollen tube growth was observed under UV light using a microscope (Keyence Bz-8000). In vitro pollen germination was performed by spreading pollen onto agar medium containing salts, sorbitol, and Suc according to (Fan et al., 2001). After an overnight incubation, pollen tubes were visible and the percentage of pollen germination was determined. Means of biological repetitions were calculated and statistical analysis performed by the *t* test. The pollen in vitro germination assay was partly modified by adding 50 μM FeSO_4 or 2 μM Zn SO_4 as indicated in the text.

Accession Numbers

Sequence data from this article can be found in the Arabidopsis Genome Initiative or GenBank/EMBL databases under the following accession numbers: *NAS1*, At5g04950; *NAS2*, At5g56080; *NAS3*, At1g09240; *NAS4*, At1g56430; *FRD3*, At3g08040; *YSL1*, At4g24120; *YSL2*, At5g24380; *YSL3*, At5g53550; *FER1*, At5g01600; *IRT1*, At4g19690; *FRO2*, At1g01580; *FIT*, At2g28160; and *ZIP4*, At1g10970.

Supplemental Data

The following materials are available in the online version of this article.

Supplemental Figure 1. Increased Fe Deficiency Gene Expression in Roots of *nas4x-2*.

Supplemental Figure 2. Fe Accumulated in Leaves of *nas4x-2* but Not in Leaves of *frd3 nas4x-2*.

Supplemental Figure 3. Fe Accumulated in Roots of *nas4x-2* and *frd3 nas4x-2*.

Supplemental Figure 4. Malate, 2-Oxoglutarate, and Succinate Contents Were Not Affected by *frd3* and *nas4x-2* Mutations.

Supplemental Figure 5. Perls Fe Staining Signals in Sections of Wild-Type and *nas4x-2* Leaves.

Supplemental Figure 6. *nas4x-2* Plants Were Late-Flowering.

Supplemental Figure 7. *NAS* Genes Were Not Expressed in Wild-Type Carpels and Stamen.

Supplemental Figure 8. *nas4x-2* Sterility Was Rescued by Fe and a Combination of Fe and Zn Spraying.

ACKNOWLEDGMENTS

P.B. and M.S. thank the Deutsche Forschungsgemeinschaft for funding in the Arabidopsis Functional Genomics Network program (Deutsche Forschungsgemeinschaft Grant Ba 1610/6-1). The work performed by R.R.-Á. and J.A. was supported by the Spanish Ministry of Science and Innovation (Project AGL2010-16515 cofinanced by European Fund for Regional Development [Fondo Europeo de Desarrollo Regional]). We thank Christine Zehren and Angelika Anna (Saarland University) for excellent technical assistance. We thank María Herrero (Estación Experimental de Aula Dei-Consejo Superior de Investigaciones Científicas, Spain) for helpful comments on floral biology. We thank Rumen Ivanov (Saarland University) for help with aniline blue staining and for useful comments on the article. We thank Nico von Wiren (IPK Gatersleben, Germany) for helpful suggestions regarding xylem sap collection.

AUTHOR CONTRIBUTIONS

M.S. was involved in research design, performed all research, analyzed data, and wrote the article. R.R.-Á. and J.A. contributed analytic tools regarding xylem sap analysis, analyzed data, and made constructive suggestions for the article. C.F.-S. contributed analytic tools regarding the determination of Fe contents. P.B. designed the research, analyzed data, and wrote the article.

Received April 5, 2012; revised May 4, 2012; accepted May 26, 2012; published June 15, 2012.

REFERENCES

- Anderegg, G., and Ripperger, H.** (1989). Correlation between metal complex formation and biological activity of nicotianamine analogues. *J. Chem. Soc. Chem. Comm.* **10**: 647–650.
- Bauer, P., Thiel, T., Klatte, M., Berczky, Z., Brumbarova, T., Hell, R., and Grosse, I.** (2004). Analysis of sequence, map position, and gene expression reveals conserved essential genes for iron uptake in Arabidopsis and tomato. *Plant Physiol.* **136**: 4169–4183.
- Becker, R., Fritz, E., and Manteuffel, R.** (1995). Subcellular localization and characterization of excessive iron in the nicotianamineless tomato mutant *chloronerva*. *Plant Physiol.* **108**: 269–275.
- Cassin, G., Mari, S., Curie, C., Briat, J.F., and Czernic, P.** (2009). Increased sensitivity to iron deficiency in *Arabidopsis thaliana* overaccumulating nicotianamine. *J. Exp. Bot.* **60**: 1249–1259.
- Chu, H.H., Chiecko, J., Punshon, T., Lanzirotti, A., Lahner, B., Salt, D.E., and Walker, E.L.** (2010). Successful reproduction requires the function of Arabidopsis Yellow Stripe-Like1 and Yellow Stripe-Like3 metal-nicotianamine transporters in both vegetative and reproductive structures. *Plant Physiol.* **154**: 197–210.
- Conte, S.S., and Walker, E.L.** (2011). Transporters contributing to iron trafficking in plants. *Mol. Plant* **4**: 464–476.
- Crawford, B.C., Ditta, G., and Yanofsky, M.F.** (2007). The *NTT* gene is required for transmitting-tract development in carpels of *Arabidopsis thaliana*. *Curr. Biol.* **17**: 1101–1108.
- Crawford, B.C., and Yanofsky, M.F.** (2008). The formation and function of the female reproductive tract in flowering plants. *Curr. Biol.* **18**: R972–R978.
- Crawford, B.C., and Yanofsky, M.F.** (2011). HALF FILLED promotes reproductive tract development and fertilization efficiency in *Arabidopsis thaliana*. *Development* **138**: 2999–3009.
- Curie, C., Cassin, G., Couch, D., Divol, F., Higuchi, K., Le Jean, M., Misson, J., Schikora, A., Czernic, P., and Mari, S.** (2009). Metal movement within the plant: contribution of nicotianamine and yellow stripe 1-like transporters. *Ann. Bot. (Lond.)* **103**: 1–11.
- Curie, C., Panaviene, Z., Loulergue, C., Dellaporta, S.L., Briat, J.F., and Walker, E.L.** (2001). Maize *yellow stripe1* encodes a membrane protein directly involved in Fe(III) uptake. *Nature* **409**: 346–349.
- de Benoist, B., McLean, E., Egli, I., and Cogswell, M., eds** (2008). *Worldwide Prevalence of Anaemia 1993–2005*. (Geneva, Switzerland: World Health Organization).
- Deinlein, U., Weber, M., Schmidt, H., Rensch, S., Trampczynska, A., Hansen, T.H., Husted, S., Schjoerring, J.K., Talke, I.N., Krämer, U., and Clemens, S.** (2012). Elevated nicotianamine levels in *Arabidopsis halleri* roots play a key role in zinc hyperaccumulation. *Plant Cell* **24**: 708–723.
- DiDonato, R.J.J., Jr., Roberts, L.A., Sanderson, T., Easley, R.B., and Walker, E.L.** (2004). *Arabidopsis* Yellow Stripe-Like2 (*YSL2*): A metal-regulated gene encoding a plasma membrane transporter of nicotianamine-metal complexes. *Plant J.* **39**: 403–414.
- Douchkov, D., Gryczka, C., Stephan, U.W., Hell, R., and Baumlein, H.** (2005). Ectopic expression of nicotianamine synthase genes results in improved iron accumulation and increased nickel tolerance in transgenic tobacco. *Plant Cell Environ.* **28**: 365–374.
- Douchkov, D., Hell, R., Stephan, U.W., and Baumlein, H.** (2001). Increased iron efficiency in transgenic plants due to ectopic expression of nicotianamine synthase. *Plant Nutr.* **92**: 54–55.
- Durrett, T.P., Gassmann, W., and Rogers, E.E.** (2007). The *FRD3*-mediated efflux of citrate into the root vasculature is necessary for efficient iron translocation. *Plant Physiol.* **144**: 197–205.
- Fan, L.M., Wang, Y.F., Wang, H., and Wu, W.H.** (2001). *In vitro* Arabidopsis pollen germination and characterization of the inward potassium currents in Arabidopsis pollen grain protoplasts. *J. Exp. Bot.* **52**: 1603–1614.
- Green, L.S., and Rogers, E.E.** (2004). *FRD3* controls iron localization in Arabidopsis. *Plant Physiol.* **136**: 2523–2531.
- Grotz, N., Fox, T., Connolly, E., Park, W., Guerinot, M.L., and Eide, D.** (1998). Identification of a family of zinc transporter genes from Arabidopsis that respond to zinc deficiency. *Proc. Natl. Acad. Sci. USA* **95**: 7220–7224.
- Guerinot, M.L.** (2000). The ZIP family of metal transporters. *Biochim. Biophys. Acta* **1465**: 190–198.
- Haydon, M.J., Kawachi, M., Wirtz, M., Hillmer, S., Hell, R., and Krämer, U.** (2012). Vacuolar nicotianamine has critical and distinct roles under iron deficiency and for zinc sequestration in *Arabidopsis*. *Plant Cell* **24**: 724–737.
- Hell, R., and Stephan, U.W.** (2003). Iron uptake, trafficking and homeostasis in plants. *Planta* **216**: 541–551.
- Herbik, A., Koch, G., Mock, H.P., Dushkov, D., Czihal, A., Thielmann, J., Stephan, U.W., and Bäumllein, H.** (1999). Isolation, characterization and cDNA cloning of nicotianamine synthase from barley. A key enzyme for iron homeostasis in plants. *Eur. J. Biochem.* **265**: 231–239.
- Higuchi, K., Suzuki, K., Nakanishi, H., Yamaguchi, H., Nishizawa, N.K., and Mori, S.** (1999). Cloning of nicotianamine synthase

- genes, novel genes involved in the biosynthesis of phytosiderophores. *Plant Physiol.* **119**: 471–480.
- Ishimaru, Y., Masuda, H., Bashir, K., Inoue, H., Tsukamoto, T., Takahashi, M., Nakanishi, H., Aoki, N., Hirose, T., Ohsugi, R., and Nishizawa, N.K.** (2010). Rice metal-nicotianamine transporter, OsYSL2, is required for the long-distance transport of iron and manganese. *Plant J.* **62**: 379–390.
- Johnson, A.A., Kyriacou, B., Callahan, D.L., Carruthers, L., Stangoulis, J., Lombi, E., and Tester, M.** (2011). Constitutive overexpression of the OsNAS gene family reveals single-gene strategies for effective iron- and zinc-biofortification of rice endosperm. *PLoS ONE* **6**: e24476.
- Johnson-Brousseau, S.A., and McCormick, S.** (2004). A compendium of methods useful for characterizing Arabidopsis pollen mutants and gametophytically-expressed genes. *Plant J.* **39**: 761–775.
- Johri, B.M., and Vasil, I.K.** (1961). Physiology of pollen. *Bot. Rev.* **27**: 325–381.
- Kim, S., Dong, J., and Lord, E.M.** (2004). Pollen tube guidance: the role of adhesion and chemotropic molecules. *Curr. Top. Dev. Biol.* **61**: 61–79.
- Klatte, M., and Bauer, P.** (2009). Accurate real-time reverse transcription quantitative PCR. *Methods Mol. Biol.* **479**: 61–77.
- Klatte, M., Schuler, M., Wirtz, M., Fink-Straube, C., Hell, R., and Bauer, P.** (2009). The analysis of Arabidopsis nicotianamine synthase mutants reveals functions for nicotianamine in seed iron loading and iron deficiency responses. *Plant Physiol.* **150**: 257–271.
- Koike, S., Inoue, H., Mizuno, D., Takahashi, M., Nakanishi, H., Mori, S., and Nishizawa, N.K.** (2004). OsYSL2 is a rice metal-nicotianamine transporter that is regulated by iron and expressed in the phloem. *Plant J.* **39**: 415–424.
- Kruger, C., Berkowitz, O., Stephan, U.W., and Hell, R.** (2002). A metal-binding member of the late embryogenesis abundant protein family transports iron in the phloem of *Ricinus communis* L. *J. Biol. Chem.* **277**: 25062–25069.
- Lee, S., Jeon, U.S., Lee, S.J., Kim, Y.-K., Persson, D.P., Husted, S., Schjørring, J.K., Kakei, Y., Masuda, H., Nishizawa, N.K., and An, G.** (2009). Iron fortification of rice seeds through activation of the nicotianamine synthase gene. *Proc. Natl. Acad. Sci. USA* **106**: 22014–22019.
- Le Jean, M., Schikora, A., Mari, S., Briat, J.F., and Curie, C.** (2005). A loss-of-function mutation in *AtYSL1* reveals its role in iron and nicotianamine seed loading. *Plant J.* **44**: 769–782.
- Mukherjee, I., Campbell, N.H., Ash, J.S., and Connolly, E.L.** (2006). Expression profiling of the Arabidopsis ferric chelate reductase (FRO) gene family reveals differential regulation by iron and copper. *Planta* **223**: 1178–1190.
- Nishiyama, R., Kato, M., Nagata, S., Yanagisawa, S., and Yoneyama, T.** (2012). Identification of Zn-nicotianamine and Fe-2'-deoxymugineic acid in the phloem sap from rice plants (*Oryza sativa* L.). *Plant Cell Physiol.* **53**: 381–390.
- Palmer, C.M., and Guerinot, M.L.** (2009). Facing the challenges of Cu, Fe and Zn homeostasis in plants. *Nat. Chem. Biol.* **5**: 333–340.
- Petit, J.M., van Wuytswinkel, O., Briat, J.F., and Lobréaux, S.** (2001). Characterization of an iron-dependent regulatory sequence involved in the transcriptional control of *AtFer1* and *ZmFer1* plant ferritin genes by iron. *J. Biol. Chem.* **276**: 5584–5590.
- Pich, A., Hillmer, S., Manteuffel, R., and Scholz, G.** (1997). First immunohistochemical localization of the endogenous Fe²⁺-chelator nicotianamine. *J. Exp. Bot.* **48**: 759–769.
- Ravet, K., Touraine, B., Boucherez, J., Briat, J.F., Gaymard, F., and Cellier, F.** (2009). Ferritins control interaction between iron homeostasis and oxidative stress in Arabidopsis. *Plant J.* **57**: 400–412.
- Reichman, S.M., and Parker, D.R.** (2002). Revisiting the metal-binding chemistry of nicotianamine and 2'-deoxymugineic acid. Implications for iron nutrition in strategy II plants. *Plant Physiol.* **129**: 1435–1438.
- Rellán-Alvarez, R., Abadía, J., and Alvarez-Fernández, A.** (2008). Formation of metal-nicotianamine complexes as affected by pH, ligand exchange with citrate and metal exchange. A study by electrospray ionization time-of-flight mass spectrometry. *Rapid Commun. Mass Spectrom.* **22**: 1553–1562.
- Rellán-Alvarez, R., López-Gomollón, S., Abadía, J., and Álvarez-Fernández, A.** (2011). Development of a new high-performance liquid chromatography-electrospray ionization time-of-flight mass spectrometry method for the determination of low molecular mass organic acids in plant tissue extracts. *J. Agric. Food Chem.* **59**: 6864–6870.
- Rogers, E.E., and Guerinot, M.L.** (2002). FRD3, a member of the multidrug and toxin efflux family, controls iron deficiency responses in *Arabidopsis*. *Plant Cell* **14**: 1787–1799.
- Roschztardt, H., Séguéla-Arnaud, M., Briat, J.F., Vert, G., and Curie, C.** (2011). The FRD3 citrate effluxer promotes iron nutrition between sympastically disconnected tissues throughout *Arabidopsis* development. *Plant Cell* **23**: 2725–2737.
- Rounds, C.M., Hepler, P.K., Fuller, S.J., and Winship, L.J.** (2010). Oscillatory growth in lily pollen tubes does not require aerobic energy metabolism. *Plant Physiol.* **152**: 736–746.
- Schaaf, G., Schikora, A., Häberle, J., Vert, G., Ludewig, U., Briat, J.F., Curie, C., and von Wirén, N.** (2005). A putative function for the arabidopsis Fe-Phytosiderophore transporter homolog AtYSL2 in Fe and Zn homeostasis. *Plant Cell Physiol.* **46**: 762–774.
- Schmidke, I., Kruger, C., Frommichen, R., Scholz, G., and Stephan, U.W.** (1999). Phloem loading and transport characteristics of iron in interaction with plant-endogenous ligands in castor bean seedlings. *Physiol. Plant.* **106**: 82–89.
- Schmiedeberg, L., Krüger, C., Stephan, U.W., Bäuml, H., and Hell, R.** (2003). Synthesis and proof-of-function of a [¹⁴C]-labelled form of the plant iron chelator nicotianamine using recombinant nicotianamine synthase from barley. *Physiol. Plant.* **118**: 430–438.
- Scholz, G., Becker, R., Pich, A., and Stephan, U.W.** (1992). Nicotianamine - A common constituent of strategy-I and strategy-II of iron acquisition by plants—a review. *J. Plant Nutr.* **15**: 1647–1665.
- Schuler, M., Keller, A., Backes, C., Philipp, K., Lenhof, H.P., and Bauer, P.** (2011). Transcriptome analysis by GeneTrail revealed regulation of functional categories in response to alterations of iron homeostasis in *Arabidopsis thaliana*. *BMC Plant Biol.* **11**: 87.
- Shojima, S., Nishizawa, N.K., Fushiya, S., Nozoe, S., Irifune, T., and Mori, S.** (1990). Biosynthesis of phytosiderophores: *In vitro* biosynthesis of 2'-deoxymugineic acid from L-methionine and nicotianamine. *Plant Physiol.* **93**: 1497–1503.
- Shojima, S., Nishizawa, N.K., and Mori, S.** (1989). Establishment of a cell free system for the biosynthesis of nicotianamine. *Plant Cell Physiol.* **30**: 673–677.
- Stacey, M.G., Patel, A., McClain, W.E., Mathieu, M., Remley, M., Rogers, E.E., Gassmann, W., Blevins, D.G., and Stacey, G.** (2008). The Arabidopsis AtOPT3 protein functions in metal homeostasis and movement of iron to developing seeds. *Plant Physiol.* **146**: 589–601.
- Takahashi, M., Terada, Y., Nakai, I., Nakanishi, H., Yoshimura, E., Mori, S., and Nishizawa, N.K.** (2003). Role of nicotianamine in the intracellular delivery of metals and plant reproductive development. *Plant Cell* **15**: 1263–1280.
- Tsukamoto, T., Nakanishi, H., Uchida, H., Watanabe, S., Matsuhashi, S., Mori, S., and Nishizawa, N.K.** (2009). (52)Fe translocation in barley as monitored by a positron-emitting tracer

- imaging system (PETIS): Evidence for the direct translocation of Fe from roots to young leaves via phloem. *Plant Cell Physiol.* **50**: 48–57.
- Vert, G., Grotz, N., Dédaldéchamp, F., Gaymard, F., Guerinot, M.L., Briat, J.F., and Curie, C.** (2002). IRT1, an *Arabidopsis* transporter essential for iron uptake from the soil and for plant growth. *Plant Cell* **14**: 1223–1233.
- von Wiren, N., Klair, S., Bansal, S., Briat, J.F., Khodr, H., Shioiri, T., Leigh, R.A., and Hider, R.C.** (1999). Nicotianamine chelates both FeIII and FeII. Implications for metal transport in plants. *Plant Physiol.* **119**: 1107–1114.
- Wang, H.Y., Klatter, M., Jakoby, M., Bäumllein, H., Weisshaar, B., and Bauer, P.** (2007). Iron deficiency-mediated stress regulation of four subgroup Ib *BHLH* genes in *Arabidopsis thaliana*. *Planta* **226**: 897–908.
- Waters, B.M., Chu, H.H., Didonato, R.J., Roberts, L.A., Easley, R.B., Lahner, B., Salt, D.E., and Walker, E.L.** (2006). Mutations in *Arabidopsis yellow stripe-like1* and *yellow stripe-like3* reveal their roles in metal ion homeostasis and loading of metal ions in seeds. *Plant Physiol.* **141**: 1446–1458.
- Weber, G., von Wirén, N., and Hayen, H.** (2006). Analysis of iron(II)/iron(III) phytosiderophore complexes by nano-electrospray ionization Fourier transform ion cyclotron resonance mass spectrometry. *Rapid Commun. Mass Spectrom.* **20**: 973–980.
- Wirth, J., Poletti, S., Aeschlimann, B., Yakandawala, N., Drosse, B., Osorio, S., Tohge, T., Fernie, A.R., Günther, D., Grisse, W., and Sautter, C.** (2009). Rice endosperm iron biofortification by targeted and synergistic action of nicotianamine synthase and ferritin. *Plant Biotechnol. J.* **7**: 631–644.
- Zheng, L., Cheng, Z., Ai, C., Jiang, X., Bei, X., Zheng, Y., Glahn, R.P., Welch, R.M., Miller, D.D., Lei, X.G., and Shou, H.** (2010). Nicotianamine, a novel enhancer of rice iron bioavailability to humans. *PLoS ONE* **5**: e10190.

Nicotianamine Functions in the Phloem-Based Transport of Iron to Sink Organs, in Pollen Development and Pollen Tube Growth in *Arabidopsis*

Mara Schuler, Rubén Rellán-Álvarez, Claudia Fink-Straube, Javier Abadía and Petra Bauer
Plant Cell; originally published online June 15, 2012;
DOI 10.1105/tpc.112.099077

This information is current as of June 15, 2012

Supplemental Data	http://www.plantcell.org/content/suppl/2012/06/06/tpc.112.099077.DC1.html
Permissions	https://www.copyright.com/ccc/openurl.do?sid=pd_hw1532298X&issn=1532298X&WT.mc_id=pd_hw1532298X
eTOCs	Sign up for eTOCs at: http://www.plantcell.org/cgi/alerts/ctmain
CiteTrack Alerts	Sign up for CiteTrack Alerts at: http://www.plantcell.org/cgi/alerts/ctmain
Subscription Information	Subscription Information for <i>The Plant Cell</i> and <i>Plant Physiology</i> is available at: http://www.aspb.org/publications/subscriptions.cfm